Official journal of the JHL 2689-9620
www.light-am.com

Review Open Access

Advanced optical methods and materials for fabricating 3D tissue scaffolds

Xiaobo Li[1,2], Wanping Lu[1], Xiayi Xu[1], Yintao Wang[1] and Shih-Chi Chen[1,2,*]

Abstract

Three-dimensional (3D) printing, also known as additive manufacturing (AM), has undergone a phase of rapid development in the fabrication of customizable and high-precision parts. Thanks to the advancements in 3D printing technologies, it is now a reality to print cells, growth factors, and various biocompatible materials altogether into arbitrarily complex 3D scaffolds with high degree of structural and functional similarities to the native tissue environment. Additionally, with overpowering advantages in molding efficiency, resolution, and a wide selection of applicable materials, optical 3D printing methods have undoubtedly become the most suitable approach for scaffold fabrication in tissue engineering (TE). In this paper, we first provide a comprehensive and up-to-date review of current optical 3D printing methods for scaffold fabrication, including traditional extrusion-based processes, selective laser sintering, stereolithography, and two-photon polymerization etc. Specifically, we review the optical design, materials, and representative applications, followed by fabrication performance comparison. Important metrics include fabrication precision, rate, materials, and application scenarios. Finally, we summarize and compare the advantages and disadvantages of each technique to guide readers in the optics and TE communities to select the most fitting printing approach under different application scenarios.

Keywords: 3D printing, Tissue scaffolds, Optical fabrication

Introduction

Tissue engineering (TE), as a modern scientific discipline, was first defined in 1993 by Langer as "the principles of biology and engineering to the development of functional substitutes for damaged tissue"[1]. Over the past 30 years, the development of TE has greatly benefitted from the leap of progress in areas such as biomaterials, three-dimensional (3D) printing technologies, integration of nanotechnology, stem cell technologies, and gene-editing technology. As such, the application of TE has obtained remarkable results in repairing bone defects, skin burns, nervous system, cornea replacement, cartilage, vascular disease, cosmetic procedures etc. It is widely believed that clinical medicine will be significantly transformed by the power of TE in the foreseeable future[2,3]. In Fig.1, the triad concept defines TE as: (1) the cells to produce the desired tissue, (2) the scaffolds to provide a framework and initial support for tissue growth, and (3) the signals in the form of biochemical or environmental (physical or chemical) cues, i.e., cell growth factors, that affect the cell's growth and phenotype[4–6]. Generally, TE starts with the seeding of variable cells and biological signals into a 3D scaffold, followed by adhesion, proliferation, and differentiation of cells incapsulated in the scaffold. Afterwards, the scaffold is implanted in vivo to

Correspondence: Shih-Chi Chen (scchen@mae.cuhk.edu.hk)
[1]Department of Mechanical and Automation Engineering, The Chinese University of Hong Kong, Shatin, N.T., Hong Kong SAR, China
[2]Centre for Perceptual and Interactive Intelligence, Building 17W, 17 Science Park West Avenue, Hong Kong Science Park, Pak Shek Kok, N.T., Hong Kong SAR, China
These authors contributed equally: Xiaobo Li, Wanping Lu, Xiayi Xu

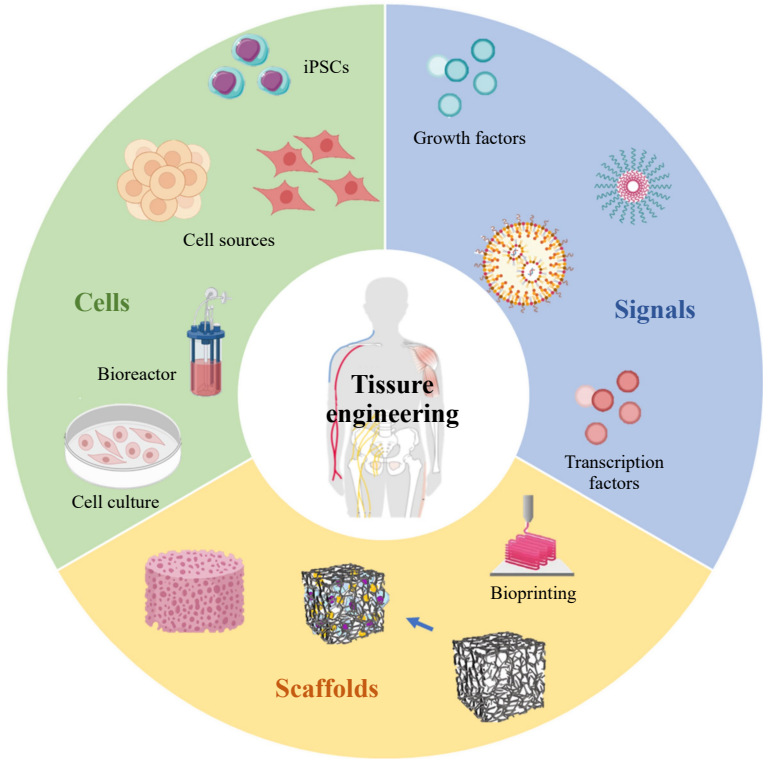

Fig. 1 Basic triad concept of TE, including cells, signals, and scaffolds.

promote tissue regeneration[7].

TE is a process of generating tissue by adding the combination of appropriate cells and materials onto the specific scaffolds[7]. However, most normal tissue-derived cells, except for certain cells such as blood cells, are anchorage-dependent and reside in the extracellular matrix (ECM)[8,9]. Further details on ECM can be found in Refs. 9, 10. Ideally, the best 3D scaffold for a given engineered tissue should be the corresponding ECM in its native states. Nevertheless, native ECMS are functionally diversified with complex composition, and naturally dynamic, making it extremely challenging to mimic such structures in vitro[9]. Therefore, a thorough investigation into scaffold fabrication is critical to enhance TE development[9,11], particularly in the fabrication of scaffolds that mimic, if not completely but at least partially, the functions of native ECM, without compromising the cell and tissue compatibility, bioactivity, and mechanical properties[12,13].

An ideal 3D scaffold that assists cell migration and infiltration requires a highly porous architecture, well-interconnected pore networks, and consistent and adequate pore size[3,12]. Over the past few decades, 3D scaffolds have been fabricated via various conventional manufacturing techniques, e.g., fiber bonding[11], phase separation[14], solvent casting[15], and membrane lamination[16]. However, these techniques all fall short of a precise control over the scaffold architecture, pore network, and pore size. Thanks to the leaping progress in 3D printing technology in the past 20 years, the fabrication of customized scaffolds with controlled structure and scale is now a reality[17–23]. Moreover, advanced 3D printing methods have enabled the printing of the fixture of cells, growth factors, and multiple biocompatible materials (both natural and synthetic) altogether onto the complex 3D scaffolds that possess a high degree of structural and functional similarities to native ECMs[2]. Fig. 2 presents some examples of 3D scaffold fabrication via different methods.

There are two distinct types of 3D printing methods: non-optical and optical[26]. The non-optical-based methods include techniques such as fused filament deposition (FFD), fused deposition modeling (FDM), electron beam melting, powder bed fusion (PBF), and partial extrusion-based printing (such as binder jetting). On the other hand, the optical-based methods include stereolithography (SLA), selective laser sintering (SLS), multiphoton stereolithography, and other extrusion-based and jetting-based printers. More details on these 3D printing methods can be found in earlier publications[27,28].

The optical method overpowers its counterpart for its

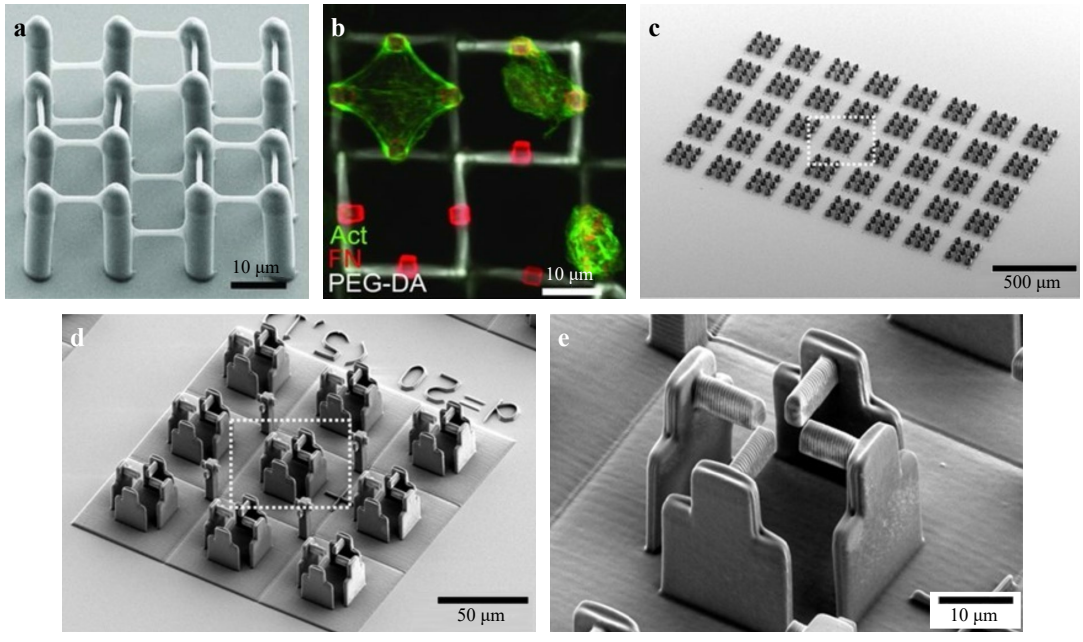

Fig. 2 a-b Cell holder (reprinted by permission from Wiley-VCH: Advanced Materials[24], copyright 2011). **c-e** Scanning electron microscopy (SEM) micrographs of a typical sample with 360 scaffolds (without the host-guest hydrogel) with increasing magnifications from left **c** to right **e**. (reprinted from AAAS: Science Advances[25], copyright 2020).

fabrication resolution, quality, reproducibility and rate as summarized below[29]:

1. As the fabrication resolution via the optical approach is determined mainly by the diffraction limit of the optical system, one can obtain a higher resolution by using a light source with shorter wavelengths and an objective with higher NA.

2. As opposed to other methods based on heat treatment and laminating, the optical method renders a firmer connection of adjacent voxels, and its post-processing step, such as photocuring, also contributes to the printing quality.

3. The optical 3D printing method is more effective in fabricating various materials, e.g., metals and alloys, ceramics, polymers, and composites, which is an important strength in scaffold fabrication where a material's specific nature, physical and chemical properties are called for to address different needs.

Based on the above advantages, the optical 3D printing method is undoubtedly the preferred method for scaffold fabrication in TE[18].

In the following sections, we first provide a comprehensive review of various optical 3D printing methods for fabricating 3D tissue scaffolds from the perspectives of the fundamentals (Section 2), materials (Section 3), and applications (Section 4.1). Secondly, we compare the performance across different fabrication technologies in terms of precision, rate, materials, and application scenarios. Finally, we recommend the most situation-appropriate method under different application scenarios (Section 4.2), followed by an outlook for the research focus in the coming years (Section 5).

Optical 3D printing methods

Optical 3D printing methods are implemented by connecting voxels and building 3D structures via light-matter interactions, which involve different physical processes, such as melting and fusing materials by heating, curing, or sintering; photo-induced cross-linking; and transferring materials via laser assisted bio-printing, etc.[30,31].

Common techniques are as follows:

1. Optical extrusion-based methods, whereby the photosensitive materials are extruded and then solidified by light exposure (such as UV). A good example is direct ink writing (DIW)[32,33].

2. Optical jetting-based methods, whereby droplets of feedstock materials are selectively sprayed and deposited, followed by light curing. Common methods include material jetting (MJ)[34,35] and polyjet printing (PJP)[36–38].

3. Laser-based methods, whereby laser is used to bond material powders, solidify fluid media[39–42], or induce cross-linking mechansms. Common techniques include SLA[43–45], SLS[46–48], and two-photon polymerization (TPP)[49,50].

In recent years, the 3D printing technology has advanced significantly thanks to the innovations brought about by the latest optical methods. In the next section, we will elaborate on these 3D printing methods, from their fundamental principles to the most advanced development.

Optical extrusion-based methods

Extrusion-based 3D printing methods play a critical role in the additive manufacturing (AM) technology due to their strengths in reproducibility, flexibility, and process control[30]. Most extrusion 3D printers are thermoplastic-based, where heated thermoplastic material, in the form of paste or thick ink, is extruded from a moving nozzle head to print 3D objects layer by layer. In recent years, extrusion 3D printing systems in TE have gained much attention due to its simple design and its capability to process a wide range of biomaterials effectively. In certain applications, such as tissue scaffold printing, additional depositing and fusing strategies need to be applied as per the materials being used. Most common extrusion-based fabrication methods include FDM, precision extrusion deposition (PED), DIW, PJP, binder jetting etc. Here we will review only light-based techniques such as DIW and PJP. Details on other extrusion-based 3D printing methods can be found in Refs. 30, 51.

DIW is one of the most prevalent extrusion methods in printing at meso- and micro-scales. Conventional DIW methods involve printing with melted materials ("ink"), i.e., polymer and wax, that is dispensed from small nozzles under controlled flow rate and then deposited along digitally defined paths to fabricate 3D structures in a line-by-line or layer-by-layer manner[32]. Recent research has focused on addressing the growing need for material diversity and biocompatibility. In 2010, Lebel et al. developed a UV-assisted DIW fabrication system that enabled continuous fabrication of 3D geometry[52]. In this system, the UV-curable nanocomposite is exposed to 365-nm UV light immediately after extrusion to enable free-form printing. However, the resolution obtained is limited at around 100 μm. Based on the same setup, a wide spectrum of materials have been printed[53–56]. In 2016, Mark et al. proposed a laser-assisted DIW, namely laser-DIW, to achieve one-step fabrication of complex 3D metal features on different substrates[33]. As the schematic shown in Fig. 3a, the UV light was replaced by a focused infrared (IR) laser with sufficient power density for metal annealing. By combining the patterning and annealing in a single step, the metallic features were printed with the requisite mechanical properties to fabricate arbitrary objects in midair with precision, hence generating complex curvilinear structures without the need for support material. The resulting metal wires (with diameters of 10 μm, 3 μm, and 600 nm) could be deposited on low-cost and soft plastic substrates such as polyethylene terephthalate (PET) films. Such method has opened up tremendous possibilities in fabricating biomedical sensors or other customized electronics in an innovative fashion.

Traditional UV-based DIW techniques controls the printed feature size by varying the power of the UV light; yet, as the curing light power increases, the resolution and structural uniformity care be significantly compromised, making multiscale parallel processing challenging. To overcome such difficulty, in 2020, Zhu et al. combined a near-infrared (NIR) laser with up-conversion nanoparticles (UCNP), as shown in Fig. 3b, and realized a curing length of over 10 cm[57]. Owing to the considerably improved NIR

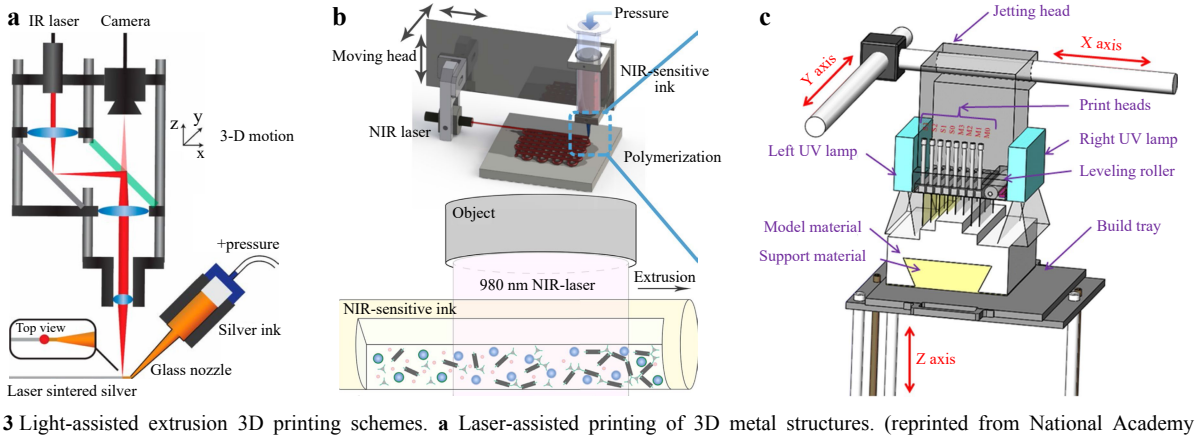

Fig. 3 Light-assisted extrusion 3D printing schemes. **a** Laser-assisted printing of 3D metal structures. (reprinted from National Academy of Sciences: Proceedings of the National Academy of Sciences[33], copyright 2016). **b** UCNP and NIR laser enabling a curing length of over 10 cm (reprinted from Springer Nature: Nature Communications[57], copyright 2020). **c** Typical PolyJet printing setup (reprinted from Springer Nature: The International Journal of Advanced Manufacturing Technology[61], copyright 2019).

laser penetration depth, this NIR-DIW method did not only solidify the deposited filament with a diameter up to 4 mm, but also demonstrated parallel manufacturing capability, which could be integrated into existing DIW systems to streamline the overall printing process.

Optical jetting-based methods

Optical jetting-based methods are an accurate AM technique in which photocurable droplets of build materials are selectively sprayed and deposited to form a designed 3D structure[58,59]. One of the most commonly used material jetting methods is PJP. As opposed to typical DIW printers, a PJP printer equipped with multiple nozzles, as shown in Fig. 3c, fabricates parts by jetting thousands of photopolymer droplets onto the build platform and solidifying them with UV light. These nozzle heads repeat the extrusion process, layer by layer, until the 3D printing process is complete[60,61]. PJP can build models with relatively high resolution and fast molding speed[62–65], and its multi-material printing capability has allowed sacrificial supporting structures in the finished model and improved the topological design for the printed device[63]. Nevertheless, the sandwich layout of the nozzle and curing lamp makes it difficult for advanced optical devices to be integrated. Therefore, recent research has more focused on enhancing the material and design. For instance, Liu et al. introduced a snap-fit method into polymer lattice design that allowed for a large-scale support-less lattice fabrication[58]. Childs et al. obtained a similar support-less result with a design where the target model was divided into two halves with an easy integration feature[65]. In contrast to the traditional approach, such design not only reduced the post-processing time by approximately 98% but also expands the possibility for broader PJP applications in 3D micro-printing.

Laser-based technologies

Stereolithography (SLA)

SLA is regarded as the first 3D printing technology in the 1980s[66]. Today, SLA, with an industry share of approximately 11% in 2021, prevails all other conventional printing technologies. SLA fabricates 3D objects based on layer-upon-layer deposition and polymerizes photosensitive resin via laser beams. SLA can be categorized into scanning (Fig. 4a) and projection (Fig. 4b) systems, based on how the laser is delivered.

In the scanning system[68,69], the stage is located below the liquid resin surface. A single laser sweeps along the resin surface, point by point and line by line, until the desired layer is completely cured. One needs to bear in mind that the thickness of the cured resin is subject to many factors, such as the exposure time, scanning rate, and laser power. To initiate the following layer, the stage sinks further into a vat until a new layer of liquid resin covers the surface and a new curing process begins[69,70]. The above process repeats itself until the whole 3D object is completely printed. However, the size of the vat constrains the height of the desired object; yet a large vat can cause additional resin waste and cleaning procedures, and besides, the serial scanning process is time consuming. For small or meso-scale printing, an inverted optical design is often adopted to achieve a more compact system envelope, which eliminates the height constraint of the printed structures and uses resins more efficiently[71]. Owing to the inverted nature, more support structures are required for certain 3D objects, which may incur additional post processing time.

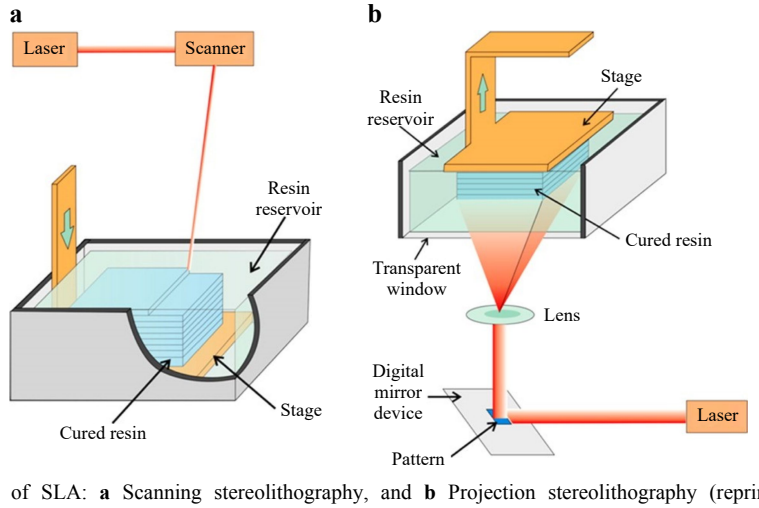

Fig. 4 Schematic illustration of SLA: **a** Scanning stereolithography, and **b** Projection stereolithography (reprinted from ACS: Analytical Chemistry[67], copyright 2014).

The projection system, also classified as digital light procession (DLP) in some literature[68,72,73], consists of the same components as the scanning system, but with a different mechanism. The digital micromirror device (DMD) in the projection system allows the whole layer to be cured simultaneously, i.e., layer-by-layer[74,75]. With DLP, the movable stage is suspended above the resin reservoir, and the light source is located under the vat. Such configuration not only removes the height restriction on the printed parts but also demands a lower volume of resin[67,76]. Though the DMD-based projection system applies the same fundamentals as the scanning system, it greatly reduces the production time due to the simultaneous use of millions of mirrors in a DMD, which cures the entire layer with a single exposure.

Among all the advanced SLA techniques, the projection micro stereolithography (PμSL) is considered a 3D printing technology that fabricates complex 3D architectures with multiple scales and materials at high resolution (up to 600 nm[67,77])[77–79]. Fig. 5a shows a large area projection micro-stereolithography (LAPμSL) developed by Zheng et al. In their design, a traditional DMD-based PμSL system was integrated with a coordinated optical scanning system. By combining a galvanometric mirror with a customized scanning lens to project the light pattern from the DMD onto the UV curable polymer resin surface, microstructures were fabricated within just a few hours of time, with feature sizes spanning over four orders of magnitude[78]. In 2018, Yang et al developed another PμSL, i.e., immersed surface accumulation-based 3D (ISA3D)[80]. By combining a dynamically controlled light beam projection with a five-axis light-guiding tool, the ISA3D printing system fabricated microstructure with 2.5 μm feature size on curved surfaces at centimeter scale. In 2020, BMF Materials Technology Co, Ltd., commercialized the PμSL system as in Fig. 5b. By adopting the multiple projection stitching process, the system offered two printing options with different resolutions and sizes: (1) 2 μm per pixel with a 50 mm × 50 mm printing area, and (2) 10 μm per pixel with 94 mm × 52 mm printing area[80]. It is worth noting that Aftab et al. proposed a high-resolution SLA with multi-scale microstructures with feature sizes ranging from 16 μm to thousands of micrometers by utilizing a static inert immiscible liquid below the resin as the constraining interface[81]. Also worth mentioning is a rapid SLA, proposed by Wakler et al., which delivered continuous printing over large areas at approximately 100 liters per hour[82]. This is the 3D printer of the largest scale ever reported in all publications. By combining liquid-crystal displays (LCD) and light-emitting diode (LED) sources, a low-cost (< US$ 500) 3D printing system has been developed, where the printing resolution is determined by the LCD pixels (20 - 50 μm); the fabrication rate is relatively low due to the low transmissivity of LCD screens[77,83].

In general, SLA-fabricated parts feature relatively high dimensional accuracy, intricate details, and smoother surface finish, making them ideal visual prototypes. However, the SLA printing process is more complicated since it necessitates support structures which need to be removed by post-processing. Besides, SLA materials are more brittle than other 3D printing materials, which is a drawback to be solved by future development in advanced materials.

Selective Laser Sintering (SLS)

SLS is an AM technique that uses high-power laser to

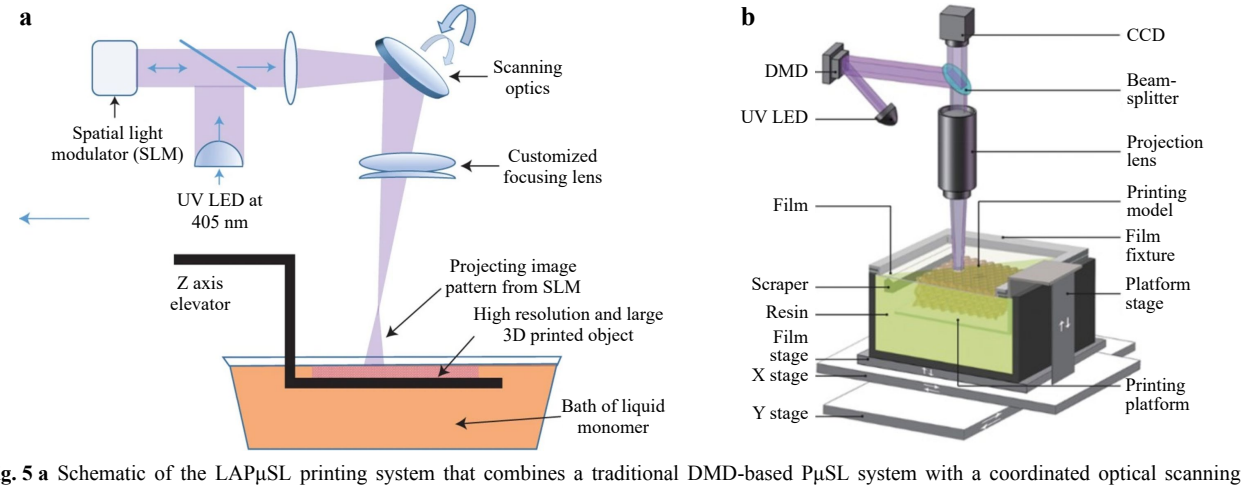

Fig. 5 a Schematic of the LAPμSL printing system that combines a traditional DMD-based PμSL system with a coordinated optical scanning system (reprinted from Macmillan Publishers: Nature materials[78], copyright 2016). **b** Schematics of LAPμSL system (reprinted from Elsevier: International Journal of Extreme Manufacturing[79], copyright 2020).

sinter small powder particles into solid 3D structures, which for example can be used to print bone scaffolds. SLS was first introduced in the early 1980s[84] and developed by Carl Deckard and Joseph Beaman in the mid-1980s[85]. Its schematic is shown in Fig. 6.

SLS shares many similarities with SLA, but rather than using resin in liquid form, SLS uses thermoplastic polymers that come in granular or powder form. Conventional SLS process includes three steps:

1. Printing: The powder is dispersed in a thin layer on top of a platform in the build chamber. By raising the temperature, the laser selectively sinters the powder surface to the melting point, and then exploits diffusion to build the parts layer-by-layer. The printing platform subsequently moves downward and fabricates a new powder layer. The process repeats itself until the whole part is complete.

2. Cooling: After printing, the build chamber cools down slightly, first inside the print enclosure and then outside the printer, so as to ensure optimal mechanical properties and to prevent warping.

3. Post-processing: The finished parts are taken out from the build chamber, separated, and removed of excess powder with compressed air or other blasting media. Unsintered powder is recycled.

SLS parts are ideal functional parts and prototypes owing to their isotropic mechanical properties. Additional support structures are unnecessary since the unsintered powder supports the part during the printing process and as a result, designs with complex geometries and shapes can be easily fabricated. Moreover, SLS enjoys a wide range of processable materials, from polymers such as polycarbonate (PC), polyvinyl chloride (PVC), acrylonitrile butadiene styrene (ABS), nylon, resin, and polyester to metal and ceramic powders. With regard to the resolution, several parameters need to be considered, e.g., the laser power and the size of the powder material. The common layer thickness is 50-200 μm, subject to micro-scale powder (typically 5-20 μm) and the laser spot size[86,87]. However, SLS parts suffer a certain degree of grainy surface finish and internal porosity, so post-processing may be necessary if surface smoothness or water tightness is required.

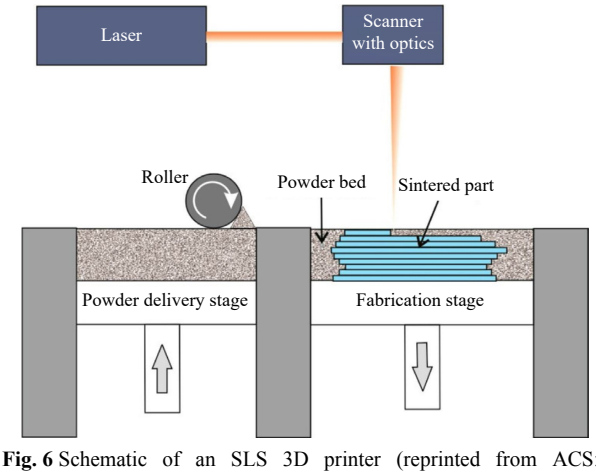

Fig. 6 Schematic of an SLS 3D printer (reprinted from ACS: Analytical Chemistry[67], copyright 2014).

To overcome these limitations, many advanced methods are thus developed[88,89]. For example, Nilabh et al. proposed a novel microscale SLS process technique, namely μ-SLS, which produced 3D metal objects with sub-5μm resolution and a throughput of greater than 60 mm^3/h[90]. One of the modifications included the use of nanoparticle (NP) inks in lieu of the microscale powder for conventional SLS process. Other improvements included an optical sub-system, where laser light was patterned via a digital micromirror array, with each pixel scaled down to nearly 1 μm.

To sum up, SLS techniques can be widely applied due to its design freedom, high productivity and throughput, low cost per part, and proven end-use materials in the market[91]. Further study on the comparison of the current commercial SLS 3D printers can be found in Ref. 92. In addition to the abovementioned laser-based 3D methods, other widely applied methods in microscale AM are all based on laser-material interaction, including Laser Chemical Vapor Deposition (LCVD[93]), laser-enabled electrochemical printing (LECP), laser-induced forward transfer (LIFT), and holographic optical tweezing process (HOTP)[94–98]. Further details on these laser-based 3D printing methods can be found in other publications[88].

Two-photon Polymerization (TPP)

TPP, another sought-after 3D printing method, resorts to ultrashort laser pulses and nonlinear optical absorption process[99]. In the liquid photoresist, the photoinitiator absorbs two photons simultaneously to release a free radical that initiates the chain reaction for polymerization within the focal volume of the ultrafast laser, enabling 3D resolved nanofabrication[100]. Following the laser irradiance and subsequent development, i.e., washing out the non-illuminated regions, the polymerized material remaining in prescribed 3D forms reaches a resolution of 100 nm or above[101,102]. In accordance with the dimension of the printing element for single exposure, different TPP systems can be created to connect voxels and print 3D structures by point-scanning, multi-point-scanning, or layer-scanning.

Though a point-scanning TPP-based 3D printing system is easy to set up with high resolution, the practicality is compromised by the low fabrication rate. An early example is a bull sculpture with an accuracy of 120 nm printed via raster scanning[103]. Point scanning can be realized via other methods, e.g., moving the sample stage[104]; based on this

approach the first 3D micromechanical component, i.e., a helix of 1.3 μm in width, was fabricated. In this design, the fabrication speed is determined by the stage. To increase the scanning speed, a common solution is to use galvanometers to perform the x- and y-axis scanning and then move the stage, e.g., the piezo stage, to change the height of the z-axis[105,106]. As such, the inertia is lower than that of the mechanical stage, thus increasing scanning speed and the control. In addition, polygonal mirrors or resonant scanners can also improve the scanning speed. For example, in 2019, Pearre et al. proposed a novel scanning method where a commercial resonance mirror was operated at 8 kHz[107] to achieve a scanning speed of 8 × 10^3 mm/s. The smallest feature size reached the order of microns. Nevertheless, the application of such design was limited owing to certain technical barriers; for example, the synchronization between a scanning device and light-switch device (e.g., electro-optic modulator) for fabricating complex 3D structures.

The fabrication speed becomes particularly important when fabricating large-volume objects. Here multi-point parallel scanning proves to be an effective method to increase the throughput. For example, one can use a micro-lens array to generate multiple laser focal points for parallel processing, while a stepping motor and a linear actuator are used for 3D scanning[108]. However, the challenge is to calibrate multiple focal points at the same time, and besides, the fixed laser focus array cannot fabricate aperiodic structures.

An alternative method to divide the incident beam into several beams is via the use of static or programmable optical diffractive elements[109,110], e.g., liquid crystal-based spatial light modulator (LC-SLM). As such, multi-point printing can be achieved by moving the stage and modulating the LC-SLM synchronously. For example, Maibohm et al. used an SLM to generate nine laser beams for parallel processing[111]. A large periodic and high aspect ratio array structure was fabricated at a writing speed of 15 μm/s and a fabrication area of several hundreds of μm^2. The finished structure was used for cell culture experiments. However, the limited LC-SLM switching rate, i.e., tens of Hertz, had an adverse effect on the printing speed and the fabrication of complex or aperiodic structures.

To achieve speed and flexibility simultaneously, or even random scanning, the DMD overpowers the SLM owing to its high pattern rate, i.e., up to 32.5 kHz, and power handling ability. When it comes to femtosecond laser imaging, the DMD-based single-point scanning and beam shaping capabilities have been proven to be highly effective[112]. Moreover, commercial DMDs are well-designed and cost-effective. Lastly, DMD-based fabrication techniques can perform random-access scanning at any position within the operational range, not to mention its high precision and high throughput[112–114]. After thoroughly investigating into the topic, our group proposed a novel multi-focus scanning method using DMDs in 3D nano-manufacturing in 2019[115]. This DMD-based scanning method can randomly generate from 1 to 100 scanning points in space, with axial and lateral scanning resolutions of 270 nm and 130 nm, respectively. Fig. 7a shows a schematic diagram of the light path of this multi-focus 3D printing system. Fig. 7b shows the printing result achieved by single-point scanning, the design of the octet truss model, and the obtained SEM image. Fig. 7c shows the scanning results of three woodpiles structures manufactured with a single focus, two foci, and three foci, respectively. The maximum parallel printing speed is 22.7 kHz or 5 mm/s. When a 40 × objective lens is used, the working volume is 103 × 206 × 524 μm^3.

Compared with single-point and multi-point scanning, the layer-by-layer scanning method reduces fabrication time at the expense of increased minimum feature size[77,116]. Although the early layer-scanning optical method, such as the PμSL in Section 2.2.1, features rapid processing time[77–79], the fabrication performance is greatly affected, i.e., disrupted speed caused by the back-and-forth switching and compromised resolution as a result of limited number of pixels. Here TPP comes into play to with its capabilities to improve processing accuracy and generate nanoscale features.

At the same time, simultaneous spatial and temporal focusing (SSTF) is proposed to disperse the laser pulses in space through a diffraction grating, and then recombine the dispersed spectrum, i.e., compress the laser pulses, at the conjugate plane, which effectively forms a femtosecond light sheet at the focal region[117,118]. The advantage of this method is that SSTF enables TPP to be performed in a layer-by-layer fashion without sacrificing the resolution. Temporal focusing has been demonstrated for both high-speed imaging and fabrication with slightly compromised resolution[117–120]. In 2019, our group proposed a femtosecond projection two-photon lithography (FP-TPL) method where a DMD was combined with temporal focusing to encode arbitrary 2D patterns on the light sheet for the fabrication of microstructures[121]. Fig. 8a–c show the process of utilizing a DMD to realize layer-by-layer printing, the optical schematic diagram, and the principle of the FP-TPL system. Fig. 8d shows the resulting structures with the best-reported throughput (10-100 mm^3/h) and resolution (140 nm/175 nm in the lateral and axial directions respectively). In this system, the maximum size of a single

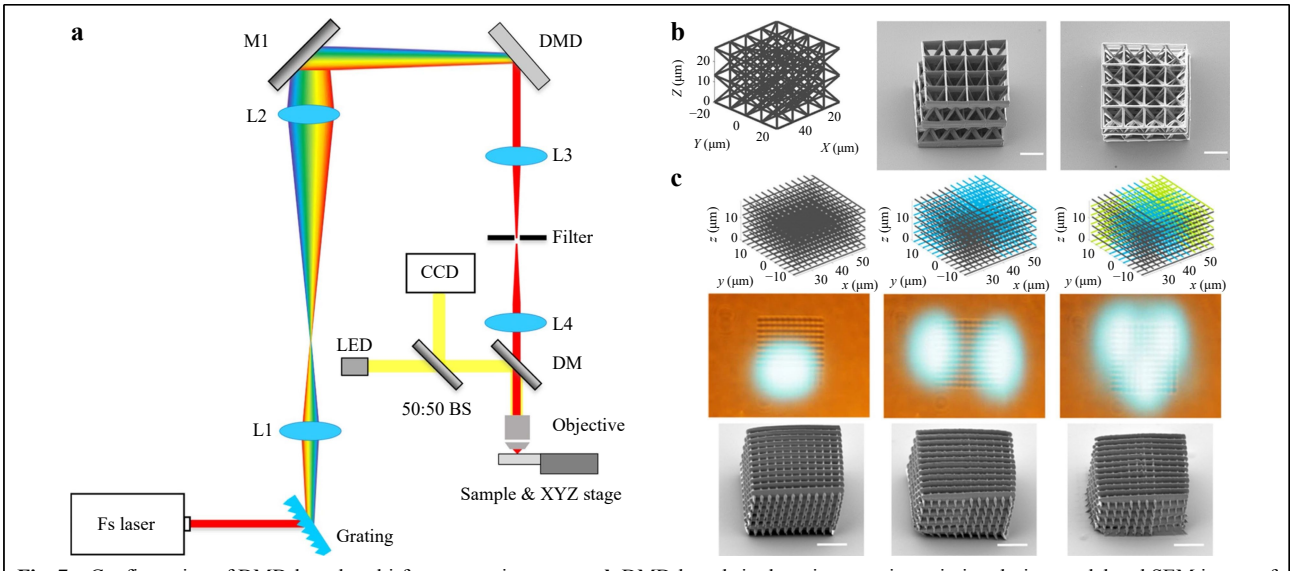

Fig. 7 a Configuration of DMD-based multi-focus scanning system. **b** DMD-based single-point scanning printing design model and SEM image of the octet truss printing result. **c** DMD-based scanning with a single focus, two foci, and three foci respectively to make woodpile structures (reprinted from Springer Nature: Nature Communications[115], copyright 2020).

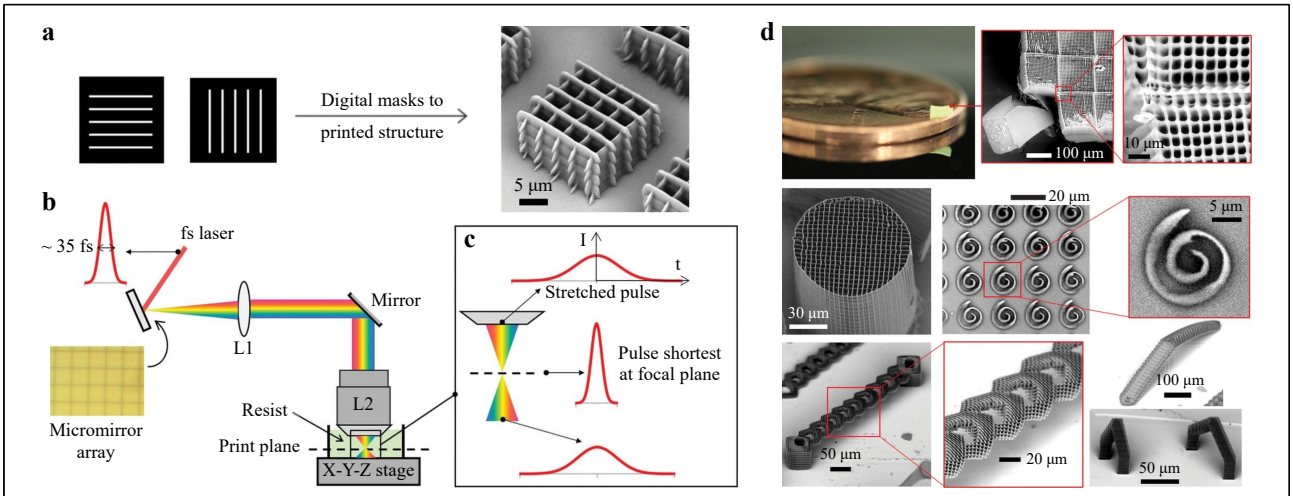

Fig. 8 a 3D printing using digital masks based with a layer-by-layer projection. **b** Schematic diagram of the optical path of the FP-TPL system. **c** Schematic diagram of temporal focusing. **d** The structure is obtained by processing with the FP-TPL system (reprinted from AAAS: Science[121], copyright 2019).

layer is 165 μm × 165 μm, and the scanning time of each layer is on the order of milliseconds; the processing speed reaches up to 1 million pixels per exposure. Compared with single-point printing, FP-TPL system improves the throughput by three orders of magnitude, making TPP suitable for large-scale fabrication applications. To the best of our knowledge, TPP-based 3D fabrication technique is the most efficient approach without having to compromise the resolution.

Optical 3D Printing with Volumetric Fabrication

Unlike point-, multi-point, or layer scanning methods, the volumetric fabrication method distinguishes itself for the control over every voxel's exposure dose or intensity in the whole 3D working space. A 3D object is formed when the power or dose at the designated position exceeds the polymerization threshold. The first volumetric fabrication method was proposed and demonstrated by Shusteff et al. in 2017[122], as illustrated in Fig. 9. They utilized the holographic patterns of light fields to control the intensity in a 3D working space. The laser power was carefully controlled to cure the resin at the designated position with high intensity, thus achieving one-step volumetric AM. As shown in Fig. 9, the optical design of the printing system included a phase-only LC-SLM, which was used to

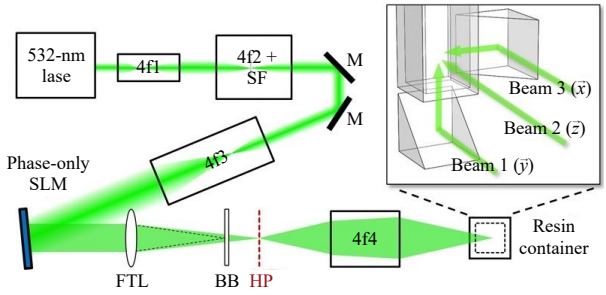

Fig. 9 Optical configuration of the holographic volumetric 3D fabrication system (reprinted from AAAS: Science Advances[122], copyright 2017).

generate holographic patterns in X-Y-Z directions. With two 45° prisms, the beams at the folded side and at the bottom intersected with the central beam in the working space. The region of the intersection was solidified, and thus formed a 3D part. This method achieved the fabrication of 3D structures at mesoscale with a single exposure within a duration of 5-10 seconds. Micro-3D printing can be achieved with the use of a beam delivery system of higher magnification.

Driven by advanced microscopies, innovative volumetric additive 3D printing methods are developed, e.g., computed axial lithography (CAL). In 2019, Bhattacharya et al. proposed a volumetric AM method via tomographic reconstruction[123], of which the printing mechanism and configuration are as shown in Fig. 10a, b. According to his design, the exposure dose was controlled by illuminating the resin at a constant rotation speed with a dynamic light pattern. Based on the target 3D structure, 2D images were calculated as a function of the rotation angle and projected serially to the rotating resin. Complex and support-less structures were thus fabricated with soft materials while obtaining superb surface smoothness. Attested as a high throughput approach, the CAL fabrication for centimeter-scale structures can take only 30-120 seconds. Nevertheless, the resolution remains limited at 300 μm due to the étendue of the light source in the projection process, which is unavoidable and may cause distortion to the printed object. In 2020, Loterie et al. proposed a tomographic system with higher feature resolution using a low-étendue illumination system[124]. They employed an integrated closed-loop feedback system, as shown in Fig. 10c, to precisely control the resin photopolymerization kinetics in the whole working space. A feedback algorithm was established to factor in the influence of light étendue, the resin viscosity and reactivity, and the tomographic reconstruction dose to achieve high resolution and fidelity. Fig. 10d shows that once the feedback was introduced, 3D structures of centimeter-scale could be fabricated within 30 seconds, while obtaining 80 μm positive and 500 μm negative feature sizes. In addition, in 2020, Regehly et al. reported an advanced volumetric AM technique, i.e., xolography, which eliminated the nonlinearities by using two intersecting light beams of different wavelengths to solidify localized regions. With such improvement, solid objects were printed with a feature resolution of up to 25 μm at a rate of up to 55 mm^3/s[125]. The resolution was also enhanced by ten times compared with other volumetric

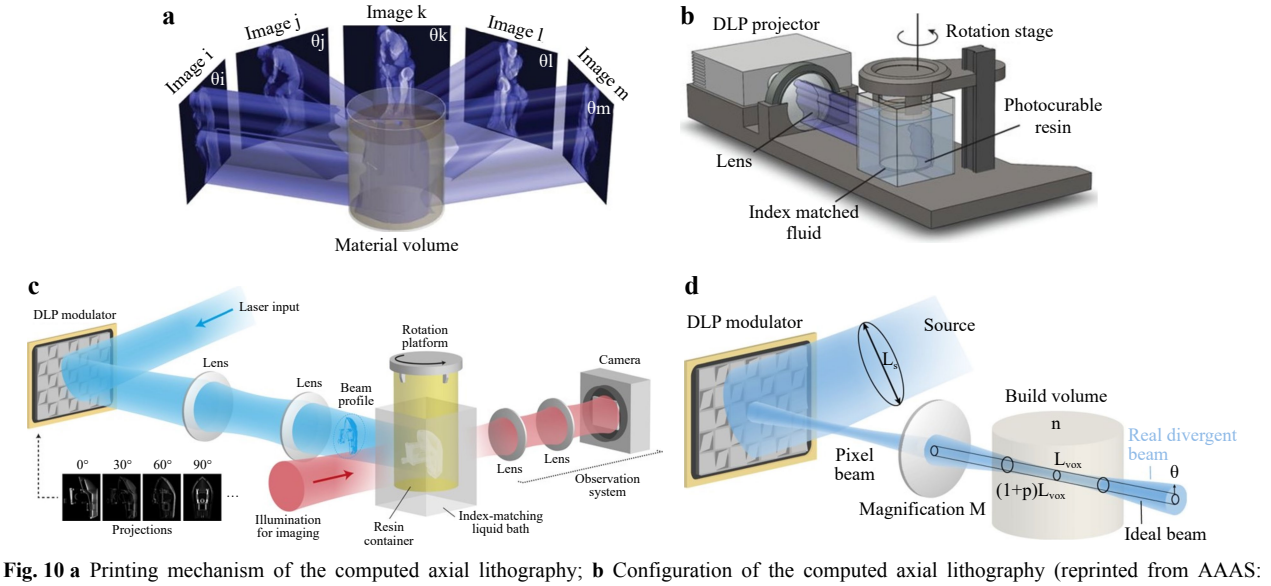

Fig. 10 a Printing mechanism of the computed axial lithography; **b** Configuration of the computed axial lithography (reprinted from AAAS: Science[123], copyright 2019). **c** Configuration of tomographic 3D fabrication system with feedback; **d** Etendue-limited optical resolution (reprinted from Springer Nature: Nature Communications[124], copyright 2020).

methods, and the volume generation rate was at least three orders of magnitude higher than TPP.

In comparison with point or layer scanning methods, the volumetric method excels in throughput, fidelity, and surface smoothness, but falls short in resolution due to the integration effect. Nevertheless, the volumetric approach has paved the path for ultrafast production of mesoscale 3D parts with precise structures.

Source materials of scaffolds fabricated by optical methods

In the TE field, the scaffold serves as a framework to support cell attachment, proliferation and migration, an extracellular matrix, and also a carrier for therapeutic cargos. Having to mimic the properties and functions of living tissues, therefore, certain criteria for scaffold design and fabrication must be factored in, i.e., biocompatibility, biodegradability, mechanical properties, biological activity, and scaffold architecture[3]. Otherwise, any random scaffold with uncontrollable morphology will not reproduce the complex and specified features of normal tissues as required[126]. In other words, one needs to have precise control over the intended scaffolds, from mimicking cellular microenvironments and regulating cell behaviors at nanometer and millimeter scales, to matching the tissue's mechanical and biochemical properties at macroscopic scales[127]. However, the design based on conventional scaffold fabrication techniques, e.g., salt-leaching, gas-foaming, phase separation, or freeze-drying, is usually constrained by the partial control over the scaffold architecture[128,129]. With the introduction of advanced optical methods, e.g., light-based extrusion, SLA, SLS and TPP, the scaffold fabrication has significantly improved in areas such as surface chemistry, morphology and microstructures, thanks to the enhancement in resolution, efficiency, automaticity, repeatability, and spatial control[130].

In the following section, we will introduce four main types of biomaterials, i.e., metals and alloys, ceramics, polymers, and composites, as well as the applicable optical methods for scaffold fabrication.

Metals and alloys

Metallic and alloyed materials have long been used in TE applications, e.g., load-bearing implants for orthopedic surgeries, due to their high mechanical strengths[131–133]. The most widely used metal and alloy in clinical applications include iron, cobalt, chromium, stainless steel, nitinol, titanium, their respective alloys, and cobalt-chromium alloys[134]. Fig. 11a displays a 3-centimeter long miniaturized human femur model fabricated with Fe-30Mn powder[135].

At present, there is only a limited number of available 3D printing methods for metallic scaffold fabrications, and among which the most common ones are SLS and selective laser melting (SLM). When applying these methods, the metal material is first deposited by a nozzle or in a powder bed, and then selectively melted and fused. The printing resolution could reach tens of microns[137,138] at a printing speed of approximately 100 cm^3/h[137]. Fig. 11b, c show an example of Ti6A14V scaffold with microrough surface resulted from the melting process, which may support cell differentiation and osseointegration[136]. Besides, these methods can print a wide range of materials based on powder and wire, including pure metal, alloy, and metal composites, and among which the most investigated are titanium alloys, aluminum alloys, cobalt-based alloys, nickel-based alloys, and stainless steel[139].

The importance of biocompatibility and corrosion resistance of metallic implants cannot be emphasized enough, for the lack of which may lead to severe infections or even life-threatening reactions[133]. At the same time, these scaffolds need to be degradable so as to yield sufficient growth space for the new tissue. Therefore, biodegradable metals (BMs) are preferred because they offer desirable degradation and compatibility in vivo, and can be readily metabolized by pathways in human body. Pure metals and alloys containing magnesium (Mg), iron/Ferrum, zinc, and calcium have been used to produce biodegradable metallic scaffolds. For example, Chou et al. discovered that the

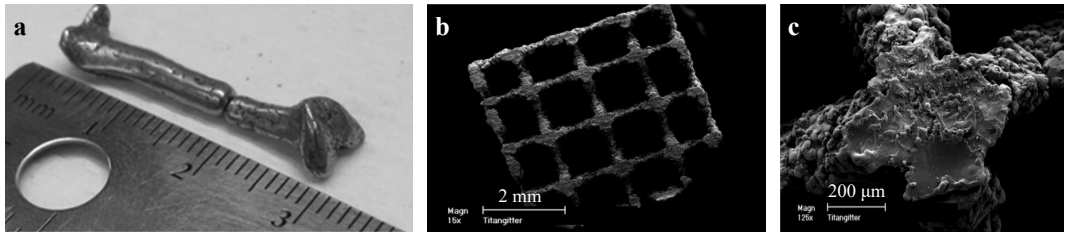

Fig. 11 a 3D printed miniaturized human femur model fabricated with Fe-30Mn powder after SLS (reprinted from Elsevier: Acta Biomaterialia[135], copyright 2013). **b**–**c** SEM images of Ti6A14V scaffolds for cell differentiation and osseointegration (reprinted from Mary Ann Liebert: TE Part C: Methods[136], copyright 2008).

iron-manganese (Fe-Mn) alloy worked well as bone scaffold materials[135]. They fabricated scaffolds with Fe-Mn as the powder bed via extrusion-based printing technique. An unspecified water-based organic solvent was used as the binder solution. The resulting Fe-Mn scaffold demonstrated strong tensile mechanical properties, similar to that of human bones, as well as satisfying biodegradability that promotes cell proliferation and bone regeneration[18]. Table 1 summarizes common metals and alloys used in TE applications. In-depth discussions on metal- and alloy-based tissue scaffolds can be found in Refs. 140–142.

Ceramics

Ceramics are characterized by high mechanical stiffness, low elasticity and high brittleness[3]. Ceramic-based scaffolds with hard tissues are exceptionally biocompatible and bioactive because their chemical structures mimic the mineral phase of native bones. In dental and orthopedic practice, ceramics are commonly used as coating for metallic implants to repair bone defects[126].

There are two common types of bioceramics for scaffold fabrication: bioinert ceramic and bioactive ceramic. Bioinert ceramic materials mainly consist of alumina (Al_2O_3) and zirconia (ZrO_2). Because of their excellent mechanical strength and corrosion resistance[149,150], alumina and zirconia have been extensively used in the fabrication of artificial femoral heads, acetabular cups, prosthetic bearings, and dental implants[151]. The introduction of other inert materials, e.g., titanium dioxide (TiO_2) and silicon carbide (SiC)[152,153], has further prompted the clinical application, for instance, in the manufacture of micropillar array stents via inkjet printing technology[152,153]. Nevertheless, Alumina and Zirconia are not bioactive despite their biocompatibility, toughness, and low friction. As a result, bioactive ceramics such as hydroxyapatite[154], calcium silicate[155], and tricalcium phosphate (TCP)[156] with high osteoconductivity are highly demanded, as they provide mechanical support and help initiate bone generation. For example, hydroxyapatite, as the primary constituent of teeth and bones, is widely used for its capability to enhance osteoblast differentiation and proliferation[154, 157–159]. Fig. 12a, b are an example of such hydroxyapatite porous scaffold. Here it is essential to have precise control over the pore size and uniform distribution on the scaffold. Ceramic suspensions containing hydroxyapatite of different concentration are first used to create customized scaffolds, and once the dynamic properties are tested, the right ceramic suspension can be manufactured via SLA[160].

The use of ceramics in TE is limited due to its brittleness, the lack of compliance with soft tissue, and uncontrollable degradation rate. To address these challenges, different 3D printing techniques have been explored to fabricate ceramic-based scaffolds with enhanced properties[161], and among which SLS proves to be the most successful. Ceramic devices manufactured via SLS, e.g., customized cytocompatibility scaffolds, have been well received in the biomedical field. By optimizing

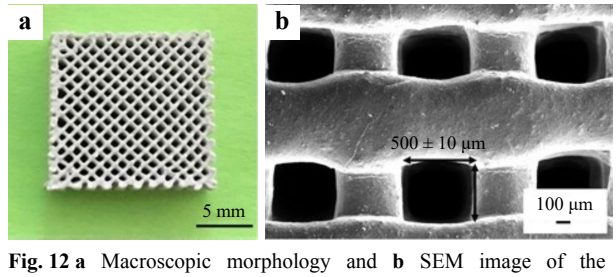

Fig. 12 a Macroscopic morphology and **b** SEM image of the hydroxyapatite porous scaffold (reprinted from Elsevier: Ceramics International[159], copyright 2019).

Table 1 Common metals and alloys for TE applications

Metals and alloys	Applications	Ref.
Mg	Implantation of magnesium alloy AZ91D open-porous scaffolds into thedistal femur condyle/condyles of the knee of rabbits.	[143, 144]
Titanium (Ti)	Implantation of powder metallurgy processed Ti13Nb13Zr porous samples into rabbit tibiae	[145]
Tantalum	Implantation of porous tantalum metaphyseal cones(Zimmer Inc. Implex, USA)into 16 patients with total knee arthoplasty.	[146]
Ti6A14V	Implantation of porous Ti6Al4V scaffold for human osteoblasts	[136]
Ni-Ti	Implantation of Ni-Ti porous superelastic cage in 62 patients (21 to 61 years) with total hip arthroplasty.	[147]
Ti-Nb-Zr-Sn	Acetabular hip cup completed with complex outer scaffold.	[148]
Metallic nanoparticles	Implantation of FeMg-NPs-containing nanoink to eradicate bone-metastatic tumor and repair the tumor-associated bone defects.	[141]

the laser power, scanning speed, scanning distance, and layer thickness, such device provides more growth space for cells and higher stent carrying capacity[162]. DIW is another effective 3D printing technique for fabricating ceramic devices; for example, a stent was printed with concentrated ceramic paste to be later used as an active element in a polymer material[163]. By adjusting the size of the pores, a scaffold made by the DIW technique that matches the size of the trabecular bone is manufactured. Such approach is considered one of the best strategies for bone repair[164]. In-depth discussions on ceramic-based tissue scaffolds can be found in Refs. 165–167.

Polymers

Polymers, unlike non-degradable metals and or ceramics, are widely used as source materials due to better processability. Polymers are unique in properties, e.g., biocompatibility, tissue-adaptability both in mechanical and physical aspects, biodegradability, stimuli responsiveness, and processability[168,169]. As a result, polymer-based scaffolds are well adopted in in vivo environment to mimic original tissue structures and functions, and to provide cell-responsive regulations. As polymer-based scaffolds are extremely versatile, fabrication methods for natural and synthetic polymers have been extensively investigated[126,170] to respond to the demands in drug delivery, wound dressings, bone and cartilage implants, or neural regeneration[171–177].

Undoubtedly, the prospect of polymers in TE application relies on successful integration of advanced optical technologies and scaffold fabrication. A recent study demonstrates that polymer crosslinked hydrogels can be bioprinted across and within the tissue of living mice by using two-photon cycloaddition, which is by far the first reported success of intravital 3D bioprinting of over 2 mm. The key to deep tissue penetration is through a precise spatial control of multiphoton microscopy and near-infrared excitation[178], as shown in Fig. 13a, b. Another example is the development of minimally invasive 4D polycarbonates scaffolds via stereolithography, where the tunable shape memory effect in 3D structures is achieved[179], as shown in Fig. 13c, d. Such breakthroughs demonstrate that with advanced optical methods, enhanced scaffolds for TE are achievable.

Natural polymers

Natural polymers used for scaffold fabrication can be classified into proteins, polysaccharides, and polynucleotides. Natural polymers such as collagen (gelatin), alginate, agarose, chitosan, and hyaluronic acid are derived from living organisms, and many of them are important ECM components[3]. In general, natural polymers-based scaffolds, being highly biocompatible, can reduce immune response, provide suitable microenvironment for cells, regulate critical signaling pathways and achieve positive tissue interactions[180]. For example, collagen is the most common protein in body and also the most critical ECM component (with gelatin as its partially hydrolyzed form, whose chemical structures are presented in Fig. 14);

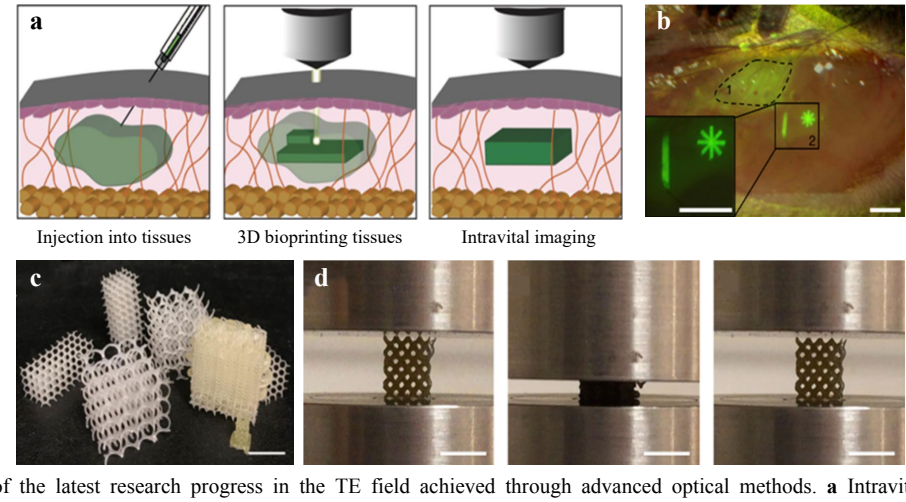

Fig. 13 Examples of the latest research progress in the TE field achieved through advanced optical methods. **a** Intravital 3D bioprinting is performed by injecting hydrogel precursor into live organs, fabrication of 3D hydrogel objects by two-photon excitation, and intravital imaging for hydrogel identification and in vivo analysis. **b** Bright-field and fluorescence stereomicroscope image of injected precursor under epimysium without (dotted line, 1) or with (continuous line, 2) hydrogel photo-crosslinking. Scale bar = 1 mm (reprinted from Springer Nature: Nature Biomedical Engineering[178], copyright 2020). **c** 4D polycarbonates photopolymerization via stereolithography for patient-specific, self-fitting scaffolds with a wide range of surface morphologies. **d** 4D scaffolds display tunable shape memory with high strain recovery (reprinted from Springer Nature: Nature Communications[179], copyright 2021).

and it can provide cellular recognition that regulates cell adhesion, proliferation and functions. Such high bioactivity is achieved through the binding sequence (Arg-Gly-Asp, RGD) naturally existed in the polymer structures of collagen and gelatin[3,181]. When collagen and gelatin are degraded by metalloproteinases in the body, new tissues are generated to replace the degraded scaffolds via cell migration[182]. Therefore, collagen and gelatin scaffolds are extensively utilized to regenerate bone, cartilage, nerve, muscles, and vasculature[183–188]. Notably, collagen and gelatin molecules can self-organize into fibrils to form hydrogels when the temperature increases to over 37 °C. This unique property gives them high printability as bioinks[189]. The combination of collagen and gelatin-based scaffolds and 3D bioprinting has great potential in fabricating artificial organs and tissues, e.g., skin, bone and cartilage, cardiovascular tissues, liver, cornea and nervous systems[189–191].

Hyaluronic acid (HA), as a biodegradable linear polysaccharide with high hydrophilicity, is also an important ECM component (Fig. 14)[192]. In fact, HA's role in wound healing, angiogenesis, and cartilage formation has been highly regarded[193], owing to the ideal interaction of bioactive HA with variable surface cell receptors (such as CD44) that induce signaling pathways to direct cell fate and promote tissue formation[194]. For example, photocrosslinkable methacrylated hyaluronic acid (MeHA) is widely used as a bioink for 3D bioprinting. To overcome the non-cell-adhesive nature of MeHA, researchers developed a hybrid bioink combining MeHA and Methacrylated gelatin (GelMA) for SLA 3D bioprinting with enhanced mechanical strength, printability, and cell-adhesive nature[195]. Table 2 summarizes common natural polymers for TE applications.

While being biologically active and biocompatible, natural polymer-based scaffolds fall short in mechanical properties, controllable degradation rate, and batch-to-batch consistency[180]. However, these drawbacks can be addressed by enhanced fabrication techniques such as cross-linking and hybridization[126]. DIW, SLA, and TPP are all common optical techniques being used in the polymerization and crosslinking process[202–207], and among which the most widely used is DIW. Burdick et al. developed a hydrogel-based DIW approach that permitted the printing of HA-based shear-thinning hydrogels directly into self-healing supporting alginate hydrogels[207]. In addition, SLA is widely adopted to fabricate porous polymer scaffolds. For example, Lam et al. used methacrylated gelatin (GelMA) and methacrylated hyaluronic acid (MeHA) as bio-inks to mimic cartilage ECM structures via SLA bioprinting approach[206]. On the other hand, TPP also emerges as a laser-based technology to prepare architecturally precise polymer scaffolds to achieve higher resolution and spatial complexity than single-photon-based methods. However, TPP presents more requirements for polymerization as opposed to

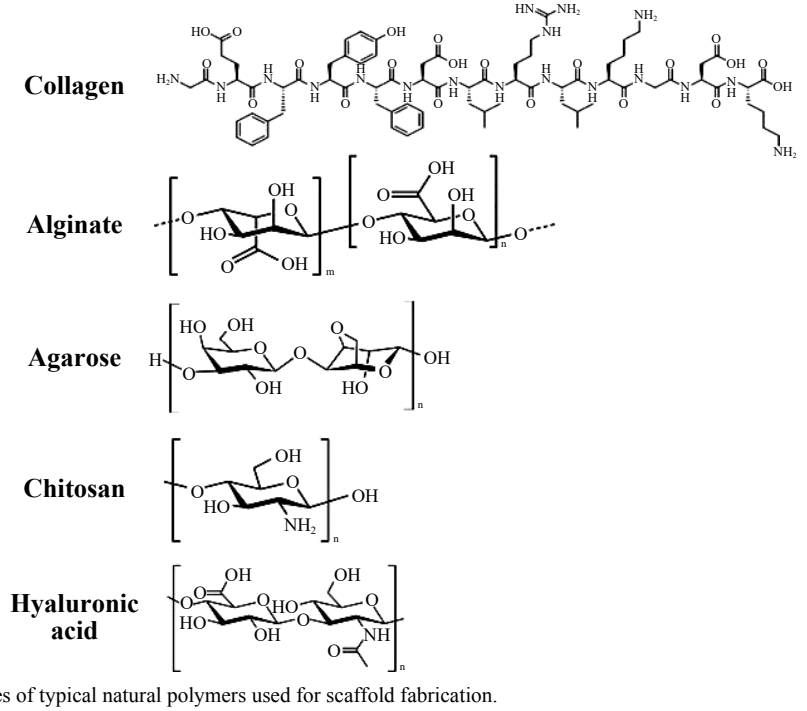

Fig. 14 Chemical structures of typical natural polymers used for scaffold fabrication.

Table 2 Common natural polymers for TE applications

Polymers	Applications	Ref.
Collagen	Regeneration of skin, bone and cartilage, cardiovascular tissues, liver, cornea and nervous systems	[189]
GelMA	Soft tissue engineering and hard tissue engineering	[191]
Alginate	Bioprinted hydrogels for bone, cartilage tissue engineering	[196]
Agarose	Carriers for cell delivery and vascular engineering	[197, 198]
Chitosan	Tissue repair and organ printing	[199]
MeHA	Tissue engineering and regenerative medicine applications	[200, 201]

single-photon polymerization, despite for the fact that any photocrosslinkable scaffold systems should be able to be fabricated via TPP in theory. Without sufficient research and understanding, only a handful of natural polymers, e.g., gelatin, HA, alginate, and albumin with acrylate or methacrylate functional groups, have been reported for scaffold fabrication[205, 208–211].

Synthetic polymers

In recent years, synthetic polymers prevail over natural polymers in scaffold fabrication, mostly for better flexibility, reproducibility, processability, batch-batch consistency, and cost effectiveness[212,213]. Although synthetic polymers lack biological cues inherently provided by many natural materials, modifications can be made to alter polymer moieties or introduce different functional groups to control degradation, regulate mechanical strength and enhance biological responses. By doing so, the application of synthetic polymer in biomedical field is considerably broadened[213,214].

Poly(ethylene glycol) (PEG), also known as poly(ethylene oxide) (PEO) is one of the most common synthetic polymer materials in TE, as shown Fig. 15[215]. Being approved by FDA, PEG is highly hydrophilic, flexible, soluble and biocompatible, thus suitable for hydrogel fabrication via variable crosslinking methods with conjugated end groups of carboxyl, thiol, or acrylate[216]. One should bear in mind that PEG and other synthetic polymers such as poly(vinyl alcohol) (PVA) and poly(acrylic acid) (PAA) are non-degradable; therefore, modifications (e.g., by conjugation of enzymatically degradable peptide) may be required[216]. On the other hand, poly(α-hydroxy acids), including poly(lactic acid) (PLA), poly(glycolic acid) (PGA), poly(caprolactone) (PCL) can be degraded by hydrolysis[217]; however, these polymers displayed extremely low hydrophilicity, which is disadvantageous for TE application where wetting ability in vivo, cell attachment and tissue interaction are critical[214].

Advanced optical methods are gaining popularity in the fabrication of synthetic polymer-based scaffold[181, 203–205]. As one of the most common synthetic polymers in TE, PEG is

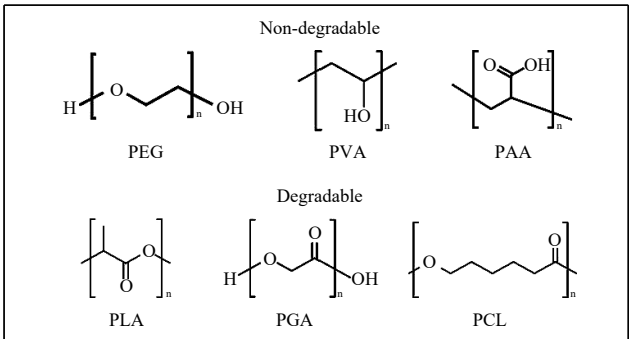

Fig. 15 Chemical structures of typical degradable and non-degradable synthetic polymers used for scaffold fabrication.

widely adopted to fabricate hydrogels via TPP to control the spatial, mechanical, temporal, and biochemical architecture of scaffolds[178,211, 218–223]. Recently, Gao et al. reported a poly(ethylene glycol) diacrylate (PEGda) hydrogel via TPP that displayed low cytotoxicity. In their study, a new kind of ionic carbazole water-soluble photoinitiator was used to achieve a low printing laser threshold of 3.7 mW and a high resolution of 180 nm. In general, the fabrication of hydrogels via TPP underlines the importance of two-photon photoinitiators with good solubility and high two-photon absorption (TPA) cross-section in the design[211]. However, a recent study reports the use of a photosensitive PEG hydrogel crosslinked by initiator-free two-photon cycloaddition to avert toxic-level concentration of photoinitiators and the release of a large number of radicals into cells and tissues[178]. Such finding will certainly propel the research in the application of radical-free and initiator-free TPP technologies. Table 3 lists selected examples of synthetic polymers used in TE applications.

Composites

Although the scaffold function can be enhanced with the use of metal, ceramic or polymer, each of these materials has its own defect that limits a more comprehensive application, e.g., metal toxicity, brittleness of ceramics, and low strength of polymers. As such, researchers start to

Table 3 Applications based on synthetic polymers.

Polymers	Applications	Ref.
PGA	Mesh networks for musculoskeletal, cardiovascular, vaginal, intestinal, lymphatic, and spinal regeneration	[224]
PPF	Scaffolds in bone TE	[225]
PEG	Scaffolds for musculoskeletal, vascular, dental pulp, and endothelial tissue regeneration	[226]
PVA	Fabrication of scaffolds for cartilage-like tissue	[226]
PPE	Biocompatible and biodegradable scaffolds for cartilage tissue	[227]
PPZ	Biodegradable scaffolds for hard TE applications	[228]

investigate different composite combinations so as to acquire the best implant solution, and it is at this point when composites come into play for scaffold fabrication via 3D printing with enhanced mechanical strengths and intricate details.

Composite scaffolds can demonstrate mechanical controllability[229] and compressive strengths as needed in the implant site, as well as enhanced bioactivity[230–232]. In fact, composites are primarily used in musculoskeletal TE, mainly bone repair, where mechanical controllability and customizability are of critical importance. The most common composites contain hydroxyapatite, TCP, or bioactive glass particles or fibers used as fillers or coatings or both in PLA, PGA, or other resorbable polymers[233,234]. For example, by adding hydroxyapatite into PLLA and PLGA, Tang et al. fabricated scaffolds for bone tissue that demonstrated better osteoconductivity, superior buffering capability and improved mechanical properties[229]. Shapiro et al. found that the composite hydrogels consisting of ceramics, for example, maintain a hydrophilic polymeric network that mimic the innate tissue, and possess good mechanical strengths to withstand the compression forces caused by cell proliferation and differentiation[233]. In fact, composites are possibly the most vital biomaterials for 3D scaffold fabrication. Table 4 lists selected examples of composite biomaterial components used in TE

Table 4 Characteristics and TE applications of composite biomaterials[234].

Bio-composite	Type	Characteristics	Application	Young's modulus
Metal and alloy	Cobalt based alloys	Mechanical properties	Neurosurgical and vascular implant fabrication, fracture fixation implant	190 – 253 GPa[235]
	Nitinol (Ni-Ti alloys)	Shape memory effect, pseudo elasticity	Dental, orthopedic, cardiovascular uses	28 – 41 GPa (Martensite) 75 – 83 GPa (Austenite)[236]
	Austenitic stainless steel	Reasonable strength, fatigue resistance	Vascular stent and electrode cardiac pacing system	200 GPa[237]
Ceramics	Bio-glass, and glass ceramics	Porosity and bioactivity	Bone defect	35 – 118 GPa[235]
	Zirconia (ZrO_2)	Mechanical properties, fracture toughness	Total hip replacement, ball head	200 GPa[238, 239]
Natural polymers	Collagen	Protein in abundance, low antigenicity, bio-compatible mechanical properties	Scaffold for soft tissue repair	0.35 MPa[240]
	Silk fibroin	Mechanical properties, bio-compatibility	Scaffold for soft tissue repair	23 KPa (collagen) 50 KPa (chitosan)[241]
	Alginate	Bio-compatible, nontoxic, biodegradable, hydrogel formation	Scaffold for cartilage repair	25 KPa[242]
Synthetic polymers	Polyethylene glycol (PEG)	Higher permeability to gases, nutrients, and metabolites, biocompatibility	Drug delivery, scaffold fabrication	470 MPa[243]
	Polycaprolactone	Slow biodegradable, structural flexibility, nontoxic metabolism of its degraded products	Scaffold for cartilage and bone matrix	2.4 GPa[244]

applications[234].

Scaffolds fabricated via optical methods: applications and future development

Applications in TE

3D cell culture

Traditionally, the study of basic life science has been profoundly benefitted from in vitro cell studies performed in 2D cell culture systems[245]. Nevertheless, the morphology and behavior of the cell growth on flat 2D surfaces is fundamentally different from those in living tissues[246], hence the concern over the accuracy and validity of these studies. As a result, biomaterial based 3D scaffolds have been developed in recent years to mimic the complex 3D tissue architecture, reflect real cell activities in ECM and enable natural intercellular interactions. Optical-based 3D printing is considered promising for customized 3D scaffolds for cell studies[247]. As mentioned in Section 2, specific 3D printing technique is selected as per the requirement and purpose of cell studies in order to fabricate scaffolds with desired compositions, morphologies, biochemical properties, and mechanical strength.

SLA is a common technology for 3D cell culture scaffold fabrication. When combined with computer-aided design, SLA can fabricate controlled and defined scaffold geometries with high resolution[18,248]. For example, Chen et al. demonstrated the use of SLA technique through mixing hydroxyapatite powder into photosensitive resin to fabricate 3D scaffold. Such scaffolds exhibited non-cytotoxicity and excellent biocompatibility[249]. SLS techniques have also been employed to prepare scaffolds from bio-compatible and bio-degradable polymers such as polyetheretherketone, polycaprolactone, and polyvinyl alcohol. Liu et al. proposed a bio-composite slurry consisting of hydroxyapatite, silica sol, and sodium tripolyphosphate to generate scaffolds using SLS[250]. These scaffolds demonstrated mechanical strength as high as 43.26 MPa, but with low porosity.

Extrusion-based printing systems, which deposits materials precisely onto a surface to form defined structures, are highly flexible in fabricating 3D scaffolds in a single-step process[246]. Materials are deposited in a layer-by-layer fashion where each layer may contain a combination of different materials. In general, commercial extrusion-based printers perform the printing of cell-laden gels, often with other polymeric materials such as metallic material and hydrogel, to yield viable and functional scaffolds[18]. In 2021, Putra et al. reported that extrusion-based 3D printing could fabricate scaffolds with porous iron with enhanced biodegradability and mechanical properties, a bone substituting biomaterial with great potentiality[251].

In addition to the abovementioned optical methods, TPP's precise and independent control of the chemical, mechanical, and geometrical properties in a printed object enables the creation of well-defined extracellular environments. For example, Ricci D et al. developed a cell culture substrate via TPP. Fig. 16 presents micro-fabricated scaffolds containing nichoid structures for the cell growth. Fig. 16a, b present a 200-μm side triangle and 300-μm side hexagonal nichoid structures with high resolution. Fig. 16c, b) present fluorescent images of human bone marrow-derived mesenchymal stem cells (stained with DAPI) seeded and cultured on the triangular and hexagonal scaffolds. Owing to unique scaffold design, the experiments demonstrated the best reported culture surface coverage rate of 88%[252].

Advanced optical methods can influence cell culture not only through dimensionality but also through dynamicity. PDMS scaffolds fabricated via TPP is one example in the study of tumor cell invasiveness. Spagnolo et al. fabricated micro scaffolds (a volume of about 50 × 50 × 50 μm^3) with

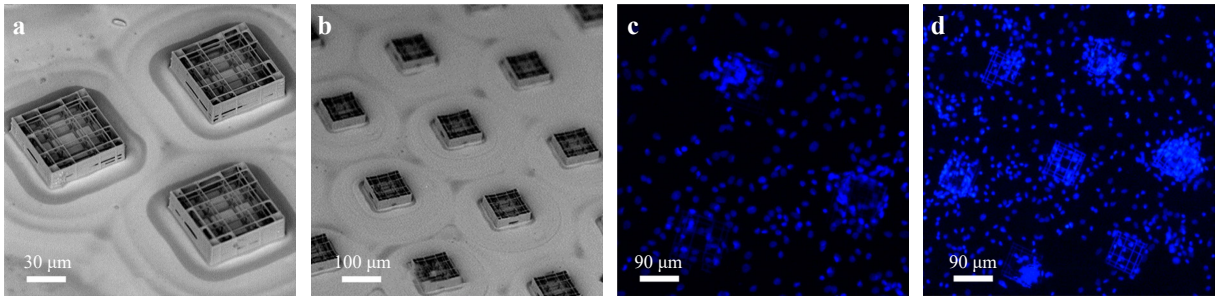

Fig. 16 SEM images of the culture substrate composed of nichoids patterned in a **a** 200-μm side triangle; **b** 300-μm side hexagonal layout. **c** and **d** Fluorescence images of cell-populated substrates. Elementary nichoids patterned in a **c** 200-μm side triangle; and **d** 300 μm side hexagonal layout. (reprinted from MDPI[252], copyright 2017).

two different pore sizes, as shown in Fig. 17a, b[253]. They used TPP to control the stiffness of microenvironments and to induce local structural variations by modulating the laser power during lithography (Fig. 17a, b), thus permitting the observation of MCF cell invasion mostly driven by soft architectures, as shown in Fig. 17c, d. Such application in architecture design via 3D printing has greatly benefitted the study in cell dynamics[253]. Recently, Rovira et al. examined different TPP design parameters to produce cell-like polyacrylate scaffolds with specific properties. These scaffolds were modified with a lipid bilayer supported on a cationic polymer to mimic human cell membranes, generating even lower critical dimensions to approximately 200 nm. Their work proved that with the selected photoresists, printing parameters, post-processing methods, greater design freedom and high resolution could be obtained at the same time, thus enabling the fabrication of biomimetic cell membranes that mimic both the shape and mechanical properties of human cells[254].

Drug delivery

Drug delivery refers to the integration of approaches, systems, technologies, and formulations that act as a medium of transport to administer therapeutics into the body to exert therapeutic effects[255,256]. The introduction of optical 3D printing methods and their applications have induced the rapid development of drug delivery technologies, from oral dosage delivery to the delivery of small drug molecules to biodegradable scaffolds for large molecules[255]. The main driving force for the rapid development lies within 3D printing's capability to fabricate drugs of customizable size, shape, and dose with precise release profiles at low cost and shortened cycle time. In this section, we will introduce a number of preeminent applications of drug delivery via optical 3D printing methods.

In 1996, Wu et al. first demonstrated the fabrication of biodegradable implants to exhibit the feasibility of drug delivery[257]. In recent years, optical based 3D printing methods have been increasingly used in pharmaceutical applications. For example, via an extrusion-based 3D printer, Khaled et al. fabricated a quick delivery tablet loaded with 80% paracetamol[258]. In 2020, Cui et al. fabricated a fast-release formulation of levetiracetam based on semi-solid extrusion printing technology achieving a loading content of 96%[259]. Laser-based 3D printing methods, such as SLA and SLS, have also been extensively applied in drug delivery applications. For example, Robles-Martinez et al. fabricated "polypills" that contain six active

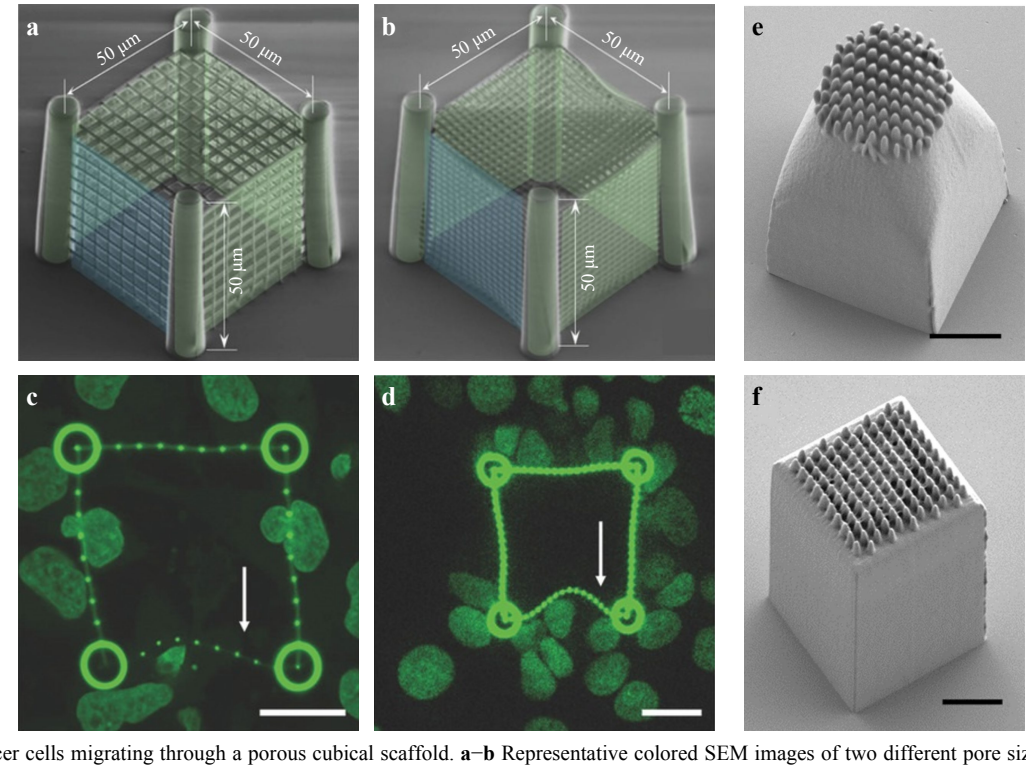

Fig. 17 Cancer cells migrating through a porous cubical scaffold. **a**–**b** Representative colored SEM images of two different pore sizes. **c**–**d** Being invaded by MCF7, cells with low stiffness facet (as indicated by the arrows) deform by the cells pushing against the cage. Scale bar: 20 μm (reprinted from Wiley: Advanced healthcare materials[253], copyright 2017). **e**–**f** Micrographs of columnar epithelial cell scaffolds printed using two configurations, scale bar: 5μm (reprinted from Elsevier: Materials & Design[254], copyright 2021).

ingredients with unique drug release profiles via an SLA printer[260]. Economidou et al. fabricated a microneedle array via SLA using biocompatible resins for transdermal insulin delivery[261]. In summary, the use of 3D printing technology in drug delivery system, especially in the application of bone TE, has been well studied in the last few decades, and the tremendous progress is proof of its potentiality. Table 5 provides a list of these applications. More details on drug delivery can be found in a separate review Ref. 262.

Bone and cartilage

Bone TE consists of scaffolds, seed cells, and cytokines. The process to repair bone defects begins with the transplantation of tissue scaffolds to the defective area, followed by the replacement of scaffold material with the growth of new bone tissues[268–270]. An ideal bone scaffold for clinical application should meet the requirements for porosity, surface area ratio, mechanical support, biocompatibility, surface activity and shape, and capability to promote cell adhesion and blood vessel and nerve growth[6,271]. Fig. 18 shows the use of 3D printing in different TE applications, which exploits a wide range of materials, e.g., metals, polymers, ceramics, or cells encapsulated within a bio-ink. One can see that 3D printing is most widely used in bone and cartilage, accounting for approximately 31% of overall application. Extrusion-based printing, a popular technique, fabricates scaffolds with bio-inks which is a mixture of one or multiple biomaterials with live cells[270]. As a form of bio-ink, hydrogels are typically used for printing cells, morphogens, and growth factors for bones and cartilages. Different formulations exist to make bio-ink hydrogels, including the seven different hydrogel formulations proposed by Bendtsen et

Table 5 Applications of 3D printing-based drug delivery.

Ref.	Material	3D printing	Drug	Applications
[262]	Hierarchical 3D-multidrug scaffolds based on nanocomposite bioceramic and PVA with Gel-Glu external coating	Extrusion	Dipyridamole and BMP-2	Bone TE
[263]	PCL 3D printing patient-specific implant, degradable porous silicon-based carriers	SLA	BMP-2	Bone graft for critical-sized bone defects.
[264]	Poly(3-hydroxybutyrate) scaffold.	SLS	Osteogenic growth peptide and its C-terminal sequence.	Bone TE.
[265]	MBG is functionalized with polydopamine and PGPL.	SLS	Dexamethasone	Osteogenic differentiation and biomineralization.
[266]	Mesoporous iron oxide nanoraspberry inside microneedles.	DLP	Minoxdil	Treatment of androgenetic alopecia.
[267]	Porous poly(ethylene glycol) dimethacrylate devices.	TPP	Rhodamine	Different biomedical applications.

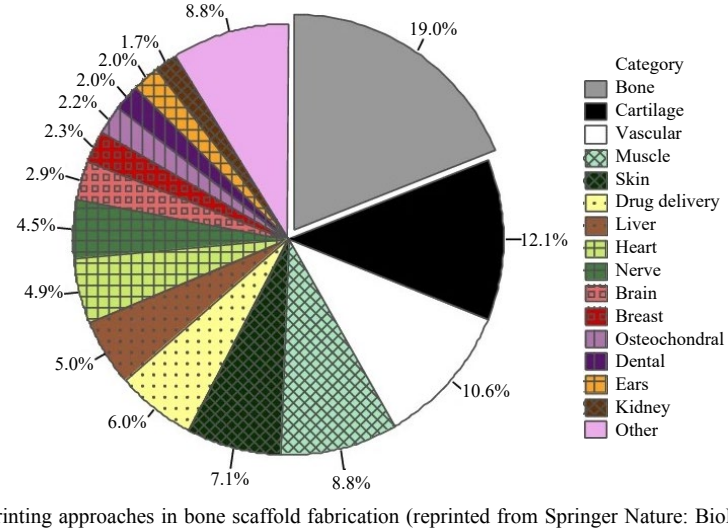

Fig. 18 Use of different 3D printing approaches in bone scaffold fabrication (reprinted from Springer Nature: BioMedical Engineering OnLine[270], copyright 2020).

al. to find the optimal composition to produce bone tissue scaffolds[272].

In addition to the extrusion-based method, SLA and SLS are proven successful in building bone tissue scaffolds from photo-cross-linkable poly (propylene fumarate) (PPF). Such scaffolds can be cross-linked through its carbon-carbon double bonds, and degraded in the body by simple hydrolysis of the ester bonds into nontoxic products[273,274]. As suggested in the study by Lee et al., on a conventional SLA machine, the UV curable polymer resin composition and laser parameters must be optimized to fabricate 3D scaffolds with controlled microstructures for specific bone TE applications. Moreover, to achieve the desired pore size and porosity, both in vitro and in vivo biological evaluations are critical for scaffold fabrication via SLA[274]. Roskies et al. used SLS technology to create a customized porous polyether ether ketone scaffold that maintained the viability of adipose and bone marrow mesenchymal stem cells and induced osteogenic differentiation of adipose-derived mesenchymal stem cells[275]. To satisfy the specific requirements for osteochondral repair, Du et al. constructed a bioinspired multilayer osteochondral scaffold consisting of poly (ε-caprolactone) and hydroxyapatite microspheres via SLS. These SLS-derived scaffolds (4 mm in diameter, 2.8 mm in thickness) exhibited excellent biocompatibility to support cell adhesion and proliferation in vitro[276].

TPP combined with the use of biodegradable polymers has great prospect in the area of micro-structured scaffold fabrication for bones. Recently, scaffolds based on cross-linked biodegradable polymers, including copolymers of lactide and e-caprolactone, have been regarded as a reliable technique for future rapid prototyping in the medical field[208,277]. For example, Timashev et al. applied TPP to fabricate hexagon-shaped scaffolds from synthetic biodegradable star-shaped polylactide (SSL) materials. These TPP-fabricated SSL scaffolds demonstrated a high Young's modulus value (> 4 GPa) with densely cross-linked structures and high spatial resolution. When loaded with human adipose-derived stem cells in vitro, the scaffold displayed excellent in vivo biocompatibility with no obvious sign of necrosis, inflammatory responses and fibrous membrane formation[210]. In 2017, Maggi et al. fabricated 3D rigid polymer scaffolds with tetrakaidekahedral periodic geometry, whose strut dimensions were on the same order as osteoblasts' focal adhesions (2 μm) and pore sizes on the order of a cell (~10 μm)[278]. A thin layer of TiO_2 was subsequently coated to ensure biocompatibility and stiffness (in the range of 0.7 – 100 MPa). Osteoblast-like cells (SAOS-2) were on these scaffolds (Fig. 19), and finally, the effectiveness was verified by tracking mineral secretions and intracellular fraction and vinculin concentrations of the cell growth after 2, 8, and 12 days in the mineralization media.

In addition to photoresist, TPP can also fabricate structures via hydrogels with high resolution and spatial complexity, which makes TPP an emerging optical process to prepare scaffolds for bones and cartilages[205,209]. For example, Felfel et al. fabricated well-defined multiphase scaffolds for bone repair via TPP by recombining hydrogel and hydroxyapatite nanoparticles. These scaffolds exhibited instantaneous shape recovery after being compressed, which is critical for arthroscopic delivery[279]. Without doubt, selecting the most suitable material for TPP process is essential to 3D scaffold fabrications due to its considerable impact on the viability and behavior of bone cell and tissue. For example, bovine chondrocytes adhere easily to woodpile scaffolds made from certain organic-

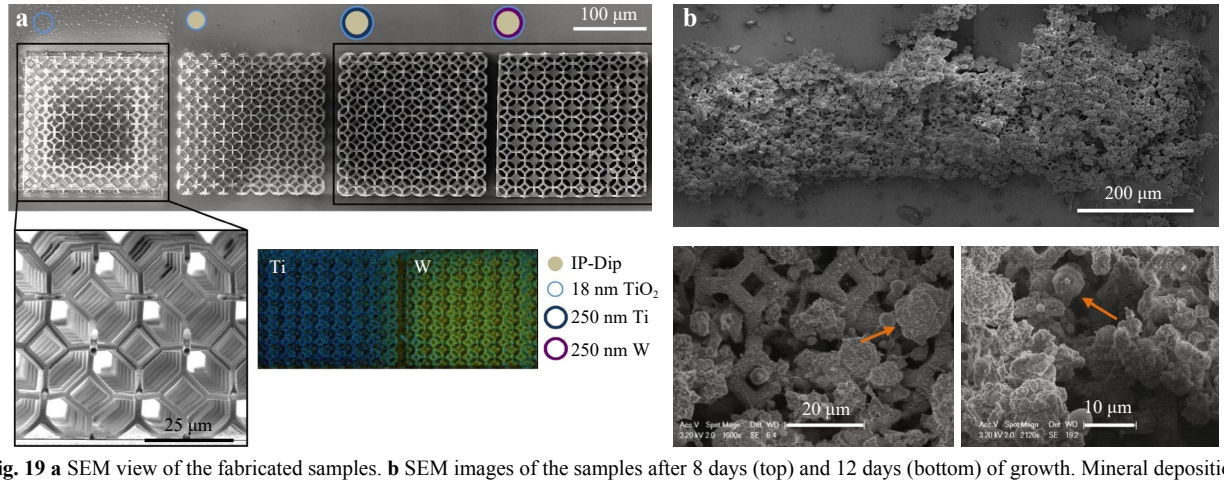

Fig. 19 a SEM view of the fabricated samples. **b** SEM images of the samples after 8 days (top) and 12 days (bottom) of growth. Mineral deposition (orange arrow) on the lattice scaffolds by Saos-2 cells (reprinted from Elsevier: Acta Biomaterialia[278], copyright 2017).

inorganic hybrid materials; they either lay or migrate on top of the scaffold or completely infiltrate into the scaffold, depending on the pore size of the woodpile[205,209]. Also, it is found that certain urethane dimethacrylates and gelatin meth acrylamides facilitated the adhesion of bovine chondrocytes on rectangular TPP-based lattice scaffolds, whereas PEGDA, with minimal cellular behavior differences, significantly prevented cell adhesion.

Others

Angiogenesis and vasculogenesis are two mechanisms through which blood vessels are formed. The sprouting blood vessels grow into the ischemic tissue in response to attractive or repulsive biochemical signals, mechanical cues, and the gradients in tissues. An interconnected vascular network is required to maintain the viability and biological function of a large growing cell population. Scaffold-based tissue regeneration, particularly with large and thick scaffolds, necessitates the incorporation of interconnected vascular network between the cells within scaffolds and the culture medium or blood, in order to facilitate the mass transfer of nutrients, signaling molecules, oxygen, growth factors, metabolic waste, etc., which manifests the core concept of TE[280,281]. Fig. 20a, b present two examples of 3D printed scaffolds for vascularization and micro-vascularization.

With regard to scaffolds for angiogenesis, biomaterial-based scaffolds fabricated via extrusion-based printing is the most prevalent. To encapsulate the vascular network and the scaffold, hydrogels or cell/peptide-loaded hydrogels are cross-linked by UV light. An example worth mentioning is the osteon-like scaffold which can be manufactured via extrusion-based 3D bioprinting to enhance the generation of cardiovascular systems[284]. From the in vitro culture study, it is found that proper cell orientation and scaffold structure can promote the generation of new blood vessels. For cardiovascular and bone regeneration, the optimal distance between cells has been found by optimizing the scaffold structure[285]; and scaffolds containing closely connected pores with a size exceeding 250 μm are essential characteristics of the stent[286,287].

Thanks to the recent advances in photolabile polymer, scaffold fabrication can be also realized via SLA/SLS approaches to address the issue of nozzle clogging and bio-ink viscosity, and ensure high-resolution printing with outstanding accuracy. For example, SLA techniques can fabricate large scaffolds with detailed vascular networks in a layer-by-layer fashion with the use of photosensitive materials and photoinitiators[13,288]. Nevertheless, laser-based methods, despite of their capability to create 3D structures with speed and precision, may cause cytotoxicity if inappropriate materials are used; therefore, they should be applied with caution and when the use of advanced biomaterials with biocompatibility is in presence.

Soft tissues connect and support surrounding tissues or organs, e.g., tendons, ligaments, blood vessels, muscles, fat, fascia, synovial membrane, and nerves. Common scaffold materials for tissue repair and regeneration are synthetic or natural polymers. Moreover, synthetic materials continue to evolve so as to ensure that biological tissues maintain their specific functions and inherent mechanical strengths. Synthetic hydrogel is a type of biomaterial suitable for manufacturing biological scaffolds due to its adjustable mechanical properties and biodegradability[289,290]. As tissue differs in size and shape, such flexibility is ideal for making soft tissue engineered scaffolds. One should bear in mind that other conditions need to be fulfilled to achieve flexibility and processing accuracy, e.g., scaffold porosity's essential role in controlling biological functions. Though achieving precise control over shape and porosity may be challenging via traditional molding methods, micro-level accuracy with stereolithography 3D printing is still attainable while simultaneously satisfying the chemical, biological, and mechanical properties in customized products[67,291]. A typical example of soft tissue reconstruction is oral soft

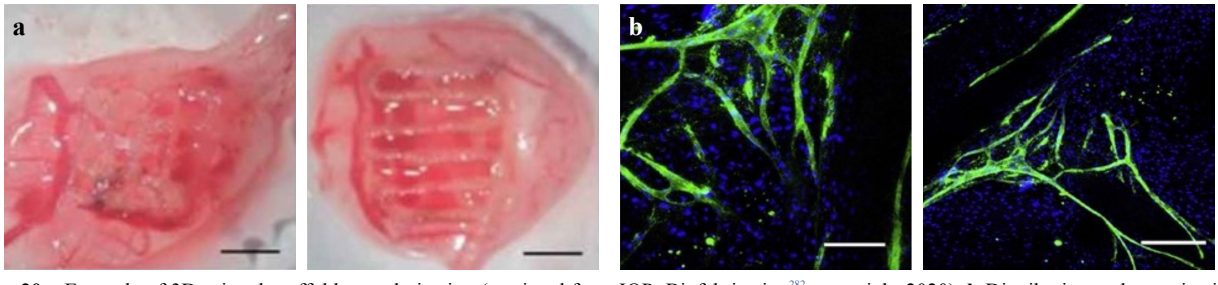

Fig. 20 a Example of 3D printed scaffold vascularization (reprinted from IOP: Biofabrication[282], copyright 2020). **b** Distribution and organization of human dermal microvascular endothelial cells and with primary human osteoblasts on fiber-mesh scaffolds (reprinted from Elsevier: Biotechnology Advances[283], copyright 2009).

tissue reconstruction, where individual oral defects can be addressed via the integration of 3D printing technology and computer-aided design.

Most common scaffolds used for soft tissue healing are hydrophilic polymers based because of their capability in forming well-defined 3D matrices that mimic the microstructure and physicochemical properties of ECM[224]. As such, the cells are exposed to an appropriate level of biomechanical stimulation, thus enhancing their physical integration into the highly hydrated body environments such as musculoskeletal, myocardium, cornea, and other soft tissues[226,292,293]. In fact, when targeting soft tissue scaffolds, SLA technique prevails optical extrusion-based or SLS methods for its capability in printing flexible and soft materials. For example, Hockaday et al. fabricated highly accurate aortic valve geometries by using SLA with PEG and alginate[294]. These scaffolds exhibited a sizeable elastic modulus range (about 5.3 ± 0.9 to 74.6 ± 1.5 kPa), accurate shape dimensions, and high viability for encapsulated porcine aortic valve interstitial cells[295].

On the other hand, one should also pay attention to the biocompatibility and toxicity issues in TE, which can be crucial, for example, when cells, biochemicals, and tissue scaffolds are simultaneously processed or printed; during such process, the effect of heating, pressure, and light-matter interaction processes can potentially influence the designed experiments adversely or sometimes favorably[296]. Recent studies on toxicity and biocompatibility of materials in TE can be found in Refs. 296–300.

Summary and recommendation

In the previous sections, we reviewed the 3D scaffold fabrication in TE from the perspectives of methods, materials, and applications. Table 6 shows the comparison across various 3D printing methods as per their respective advantages, disadvantages, fabrication rate and resolution. Fig. 21 illustrates some of the exemplary works and their respective performances. Based on these facts, we summarize and conclude that:

The extrusion/jetting based optical 3D printing method distinguishes itself in simplicity and the applicability to a wide range of biocompatible materials with outstanding throughput and fabrication rate[67,301]. It is arguably the most straightforward solution to scaffold fabrication; however, the resolution at hundred-micron level rules out the possibility of fabricating scaffolds with finer structures.

With better fabrication rate and resolution, SLA and SLS are two optical methods that dominate the present market despite of the limited resolution at micron scale[78,82,87,90,302–308]. SLA and SLS can be used to fabricate 3D scaffolds with a wide range of material options including those in liquid and solid states.

Table 6 Comparison of different optical-3D printing methods.

Methods	Materials	Rate	Resolution	Advantages	Disadvantages	Applications in TE
Extrusion/ jetting based	Polymers, Heated thermoplastic materials	4000 cm^3/h[310]	~ 100 μm	▪ Simple operation ▪ Versatile applicable materials ▪ Adaptable for bioprinting	▪ Potential toxicity ▪ Time consuming (Postprocessing)[18]	Soft tissue[311] Vascular repair[312] Drug delivery[262] Vascular scaffolds[284]
SLA	Photopolymer, (Liquid)	10^3 – 10^6 mm^3/h[122]	10 – 150 μm[313] (2 μm for LAPμSL[78])	▪ Complex internal features ▪ High resolution[67] ▪ Large part bioprinting ▪ Smooth surface finish	▪ Photopolymer required[314] ▪ Support structure required ▪ Small volume	Bone tissue[273, 274]. Drug delivery[263, 266] Vascular networks[13, 288]
SLS	Polymer, Ceramic, Metal and alloy (Powders)		50 – 200 μm (5 μm for μ-SLS[90])	▪ High mechanical properties ▪ No need for support structures ▪ Fine resolution ▪ Excellent control over microstructures	▪ Limited material selection (must be shrinkage and heat resistant) ▪ High temperature required (1.4k°C)[250] ▪ Time consuming and material wastage	Drug delivery[264, 265] Bone scaffolds[275, 276] Osteogenic differentiation[265]
TPP	Photopolymer, Hydrogel	Up to 10 – 100 mm^3/h[121]	Up to ~100 nm	▪ Very high resolution ▪ Excellent flexibility in 3D structures	▪ High cost ▪ Limited material selection	Bone and cartilage[209, 278]. Soft tissue[283] Angiogenesis and vasculogenesis[282], Drug delivery[267]
Volumetric	Photopolymers	Up to 10^3 – 10^5 mm^3/h[122, 125]	25 – 500 μm[125, 29]	▪ High fabrication rate	▪ Lower resolution ▪ Limited material selection	Being realized

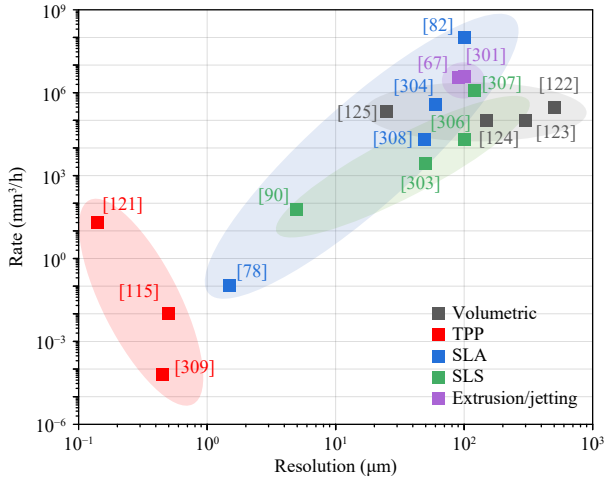

Fig. 21 Summary of different optical 3D printing methods plotted in fabricate rates versus resolution. The labels of the data point refer to the serial numbers of the corresponding references.

The TPP method, despite of slightly slower fabrication rate (10-100 mm^3/h), enjoys the best resolution, which reaches a hundred nanometers or higher[115,121,309], as well as the capability to print arbitrary 3D structures. As such, TPP technique has the greatest potential in fabricating small-scale scaffolds with complex structures. Since the range of applicable materials for TPP is limited, further studies in advanced materials and their properties are of critical importance for future advancement.

The volumetric printing method sets itself apart with fabrication rate as high as liters per hour[122–125]. Nevertheless, the approach is hindered by poor resolution and limited material selection. According to the literature, the volumetric printing method is suitable for fabricating scaffolds with pore size of several hundred microns.

Conclusion and Outlook

This paper presents an overview of the latest optical 3D printing methods that revolutionize the scaffold fabrication in TE from the perspectives of fundamental concepts, materials, and potential applications. We also examine the fabrication performance in terms of precision and fabrication rate under various scenarios, followed by recommendations for future studies in the fields of optics and TE. Optical 3D printing methods are extremely effective due to superior performance and cost-effectiveness, and the prospect of broader application depends on the breakthrough in new materials that address the fast-growing demand in 3D scaffold fabrication in TE. In fact, we recognize a positive interplay among scaffold applications, materials and 3D printing methods. In other words, the demand for advanced scaffold has been the driving force for the development in material and 3D printing methods and vice versa. Going forward, the topics of interests for future studies may include but not limited to:

A. High-throughput and fast printing solutions for scaffold fabrication

The fabrication of large-scale 3D scaffolds remains quite challenging, as optical 3D printing methods, especially TPP, achieves a much higher resolution (up to hundred nanometers) at the expense of printing time and ultimately the scaffold's final size. In a recent publication, Weisgrab et al. reported a TPP-based regenerative medicine scaffold with a large volume of 292 mm^3, yet in a processing time of 16 hours[315].

Materials and optical systems are two key elements to achieve high throughput and printing rate. First, a fast processing speed depends on photoinitiators with a high two-photon absorption cross-section (δ, with the unit of Göppert Mayer (GM)). Typical one-photon photoinitiators merely have δ values on the order of around 20-30[49], while those explicitly developed for TPP can reach 150[315]. Therefore, processing speed can be improved by developing highly efficient photoinitiators materials, and also a lower initiator concentration is preferred when fabricating biocompatible scaffolds.

Moreover, advancement in optical systems, particularly with the introduction multiple foci and volumetric fabrication, can greatly enhance the efficiency. Gittard et al. introduced an effective scaffold fabrication by TPP with multiple foci via SLM technique, as shown in Fig. 22[50,110]. Later, Zandrini et al. combined TPP with fast linear stages to produce multi-foci and thus significantly reduce the processing time by a factor of nearly five[110,224]. Finally, the FP-TPL technique developed by our team is capable of printing 3D structures with the highest throughput (10–100 mm^3/h) and resolution (140/175 nm in the lateral/axial directions) ever reported and a 90% cost reduction (~US$ 1.5 $/mm^3$) comparing with current commercial solutions[110], which may address the long-standing challenges in high-resolution large-scale scaffold fabrication.

B. Highly integrated solutions in both materials and methods

In order to further enhance the ability to mimic the complexity of ECM's physical and biochemical properties, the integration of advanced materials and methods for scaffolds need to be developed as a resort to satisfy the requirements for multi-compositional and multi-functional microstructures.

As indicated in the past research, optical-based 3D

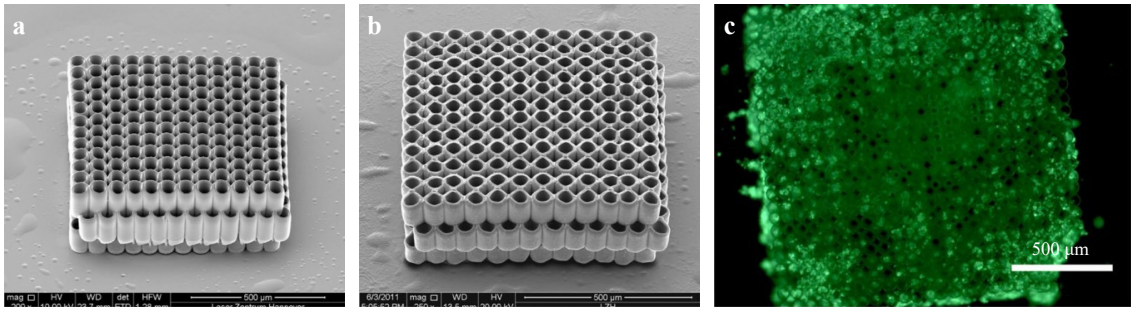

Fig. 22 Scaffolds made by TPP with **a** single focus structuring and **b** four foci structuring. **c** Image of bovine endothelial cells growing on a scaffold made by multibeam TPP (reprinted from OSA: Biomedical Optics Express[50], copyright 2011).

printing methods is capable of printing multi-material systems in which each material corresponds to distinct chemical, biological, and optical properties. For example, Klein et al. reported the first multi-material printing protocol to fabricate 3D cellular scaffolds with two materials to either promote or inhibit cellular attachments[24]. On such basis, other researchers have developed methods to print multi-material 3D microarchitectures, including cellular environments, composite metamaterials, and optical components[123,316].

However, printing with multiple materials is exceedingly more time-consuming and labor-intensive than printing with a single material due to a more sophisticated setup. To be more specific, a printer operator's skill may determine the registration accuracy for each additional material. In other words, while a multi-material system is designed with extraneous alignment structures and tolerances, the print-to-print repeatability still depends much on the user's performance; hence a higher probability of failure than that of a single-material system[316]. One solution worth exploring is to integrate a microfluidic device with TPP printers. As such, it is possible for one to fabricate multi-material and multi-functional scaffolds, and to host several cell types in accordance with the complex tissue conditions. Furthermore, by integrating actuator systems with scaffolds with multi-functional sensors, i.e., advanced fluorescent microscopy and computational imaging methods, one can also greatly enhance the analytical capabilities of fundamental and applied researches[205].

As this review covers some, if not all, of the exemplary works in the fields of 3D printing scaffolds in TE, we look forward to seeing more studies on relevant topics from both the optical and engineering communities. We believe that both the academic and industrial communities can thrive on a broadened and deeper understanding in optical 3D printing methods and its impact on scaffold fabrication in TE.

Acknowledgements

This work was supported by the Innovation and Technology Commission (ITC) (ITS/178/20FP) and Centre for Perceptual and Interactive Intelligence (CPII) Ltd under the Innovation and Technology Fund.

Author contributions

X. Li and W. Lu conducted the literature study in optical 3D printing; X. Xu and Y. Wang conducted the literature study in materials; X. Li. prepared the manuscript with input from all coauthors. S.-C. Chen supervised the project.

Conflict of interest

The authors declare no conflict of interest.

Table of abbreviations

Abbreviation	Description
3D	Three-dimensional
ABS	Acrylonitrile butadiene styrene
Al_2O_3	Alumina
AM	Additive manufacturing
BMs	Biodegradable metals
CAL	Computed axial lithography
DIW	Direct ink writing
DLP	Digital light procession
DMD	Digital micromirror device
ECM	Extracellular matrix
ECM	Extracellular matrix
FDM	Fused deposition modeling
Fe-Mn	Iron-manganese
FFD	Fused filament deposition
FP-TPL	Femtosecond projection two-photon lithography
GelMA	Methacrylated gelatin
GM	Göppert Mayer
HA	Hyaluronic acid
HOTP	Holographic optical tweezing process
IR	Infrared

ISA3D	Immersed surface accumulation-based 3D
LAPμSL	Large area projection micro-stereolithography
LED	light-emitting diode
LCD	Liquid-crystal display
LC-SLM	Liquid crystal-based spatial light modulator
LCVD	Laser Chemical Vapor Deposition
LECP	Laser-enabled electrochemical printing
LIFT	Laser-induced forward transfer
MeHA	Methacrylated hyaluronic acid
Mg	Magnesium
MJ	Material jetting
NIR	Near-infrared
NP	Nanoparticle
PAA	Poly(acrylic acid)
PBF	Powder bed fusion
PC	Polycarbonate
PCL	Poly(caprolactone)
PED	Precision extrusion deposition
PEG	Poly(ethylene glycol)
PEG	Polyethylene glycol
PEGda	Poly(ethylene glycol) diacrylate
PEO	Poly(ethylene oxide)
PET	Polyethylene terephthalate
PGA	Poly(glycolic acid)
PJP	Polyjet printing
PLA	Poly(lactic acid)
PPF	Poly (propylene fumarate)
PVA	Poly(vinyl alcohol)
PVC	Polyvinyl chloride
PμSL	Projection micro stereolithography
SiC	Silicon carbide
SLA	Stereolithography
SLS	Selective laser sintering
SLM	Selective Laser Melting
SSL	Star-shaped polylactide
SSTF	Simultaneous spatial and temporal focusing
TCP	Tricalcium phosphate
TE	Tissue engineering
TiO_2	Titanium dioxide
TPA	Two-photon absorption
TPP	Two-photon polymerization
UCNP	Up-conversion nanoparticles
ZrO_2	Zirconia

Received: 05 October 2021 Revised: 27 March 2022 Accepted: 01 April 2022
Accepted article preview online: 04 April 2022
Published online: 06 May 2022

References

1. Vacanti, J. P. & Langer, R. Tissue engineering: the design and fabrication of living replacement devices for surgical reconstruction and transplantation. *The Lancet* **354**, S32-S34 (1999).
2. Lanza, R. et al. Principles of Tissue Engineering. 5th edn. (San Diego: Academic Press, 2020).
3. O'Brien, F. J. Biomaterials & scaffolds for tissue engineering. *Materials Today* **14**, 88-95 (2011).
4. Lu, T., Li, Y., & Chen, T. Techniques for fabrication and construction of three-dimensional scaffolds for tissue engineering. *International journal of nanomedicine* **8**, 337-350 (2013).
5. Guo, B. L. & Ma, P. X. Conducting polymers for tissue engineering. *Biomacromolecules* **19**, 1764-1782 (2018).
6. Roseti, L. et al. Scaffolds for bone tissue engineering: state of the art and new perspectives. *Materials Science and Engineering:C* **78**, 1246-1262 (2017).
7. Lavik, E. & Langer, R. Tissue engineering: current state and perspectives. *Applied Microbiology and Biotechnology* **65**, 1-8 (2004).
8. Merten, O. W. Advances in cell culture: anchorage dependence. *Philosophical Transactions of the Royal Society B:Biological Sciences* **370**, 20140040 (2015).
9. Chan, B. P. & Leong, K. W. Scaffolding in tissue engineering: general approaches and tissue-specific considerations. *European Spine Journal* **17**, 467-479 (2008).
10. Muschler, G. F., Nakamoto, C. & Griffith, L. G. Engineering principles of clinical cell-based tissue engineering. *The Journal of Bone & Joint Surgery* **86**, 1541-1558 (2004).
11. Chung, S., Gamcsik, M. P. & King, M. W. Novel scaffold design with multi-grooved PLA fibers. *Biomedical Materials* **6**, 045001 (2011).
12. Pluta, K., Malina, D. & Sobczak-Kupiec, A. Scaffolds for tissue engineering. *Czasopismo Techniczne. Chemia* **112**, 89-97 (2015).
13. Migliaresi, C. & Motta, A. Scaffolds for Tissue Engineering: Biological Design, Materials, and Fabrication. (Singapore: Pan Stanford Publishing, 2014).
14. Liu, X. H. & Ma, P. X. Phase separation, pore structure, and properties of nanofibrous gelatin scaffolds. *Biomaterials* **30**, 4094-4103 (2009).
15. Sin, D. et al. Polyurethane (PU) scaffolds prepared by solvent casting/particulate leaching (SCPL) combined with centrifugation. *Materials Science and Engineering:C* **30**, 78-85 (2010).
16. Amensag, S. & McFetridge, P. S. Tuning scaffold mechanics by laminating native extracellular matrix membranes and effects on early cellular remodeling. *Journal of Biomedical Materials Research Part A* **102**, 1325-1333 (2014).
17. Yang, S. et al. The design of scaffolds for use in tissue engineering. Part I. Traditional factors. *Tissue Engineering* **7**, 679-689 (2001).
18. Do, A. V. et al. 3D printing of scaffolds for tissue regeneration applications. *Advanced Healthcare Materials* **4**, 1742-1762 (2015).
19. Zhao, P. et al. Fabrication of scaffolds in tissue engineering: a review. *Frontiers of Mechanical Engineering* **13**, 107-119 (2018).
20. Ng, W. L. et al. Deep learning for fabrication and maturation of 3D bioprinted tissues and organs. *Virtual and Physical Prototyping* **15**, 340-358 (2020).
21. Ng, W. L., Chua, C. K. & Shen, Y. F. Print me an organ! Why we are not there yet. *Progress in Polymer Science* **97**, 101145 (2019).
22. Yu, C. L. & Jiang, J. C. A perspective on using machine learning in 3D bioprinting. *International Journal of Bioprinting* **6**, 253 (2020).
23. Iandolo, D. et al. Nanoscale investigation in 3D scaffolds of cell-

material interactions for tissue-engineering. Preprint at https://www.biorxiv.org/content/10.1101/383117v1 (2018).
24. Klein, F. et al. Two-component polymer scaffolds for controlled three-dimensional cell culture. *Advanced Materials* **23**, 1341-1345 (2011).
25. Hippler, M. et al. Mechanical stimulation of single cells by reversible host-guest interactions in 3D microscaffolds. *Science Advances* **6**, eabc2648 (2020).
26. ISO. ISO/ASTM 52910.2(en) Standard practices — Guidelines for for design for additive manufacturing. Rome: ISO, 2016.
27. Chia, H. N. & Wu, B. M. Recent advances in 3D printing of biomaterials. *Journal of Biological Engineering* **9**, 4 (2015).
28. Lee, J. Y., An, J. & Chua, C. K. Fundamentals and applications of 3D printing for novel materials. *Applied Materials Today* **7**, 120-133 (2017).
29. Lin, W., Chen, D. H. & Chen, S. C. Emerging micro-additive manufacturing technologies enabled by novel optical methods. *Photonics Research* **8**, 1827-1842 (2020).
30. Gibson, I. et al. Additive Manufacturing Technologies. 3rd edn. (Cham: Springer, 2021).
31. Gebhardt, A. & Hötter, J. S. Additive Manufacturing: 3D Printing for Prototyping and Manufacturing. (Munich: Hanser Publishers, 2016).
32. Lewis, J. A. Direct ink writing of 3D functional materials. *Advanced Functional Materials* **16**, 2193-2204 (2006).
33. Skylar-Scott, M. A., Gunasekaran, S. & Lewis, J. A. Laser-assisted direct ink writing of planar and 3D metal architectures. *Proceedings of the National Academy of Sciences of the United States of America* **113**, 6137-6142 (2016).
34. Yap, Y. L. et al. Material jetting additive manufacturing: an experimental study using designed metrological benchmarks. *Precision Engineering* **50**, 275-285 (2017).
35. Moore, J. P. & Williams, C. B. Fatigue properties of parts printed by PolyJet material jetting. *Rapid Prototyping Journal* **21**, 675-685 (2015).
36. Mahajan, A., Frisbie, C. D. & Francis, L. F. Optimization of aerosol jet printing for high-resolution, high-aspect ratio silver lines. *ACS Applied Materials & Interfaces* **5**, 4856-4864 (2013).
37. Mette, A. et al. Metal aerosol jet printing for solar cell metallization. *Progress in Photovoltaics:Research and Applications* **15**, 621-627 (2007).
38. Secor, E. B. Principles of aerosol jet printing. *Flexible and Printed Electronics* **3**, 035002 (2018).
39. Wei, C. & Li, L. Recent progress and scientific challenges in multi-material additive manufacturing via laser-based powder bed fusion. *Virtual and Physical Prototyping* **16**, 347-371 (2021).
40. Xie, B. et al. Biodegradation, antibacterial performance, and cytocompatibility of a novel ZK30-Cu-Mn biomedical alloy produced by selective laser melting. *International Journal of Bioprinting* **7**, 300 (2021).
41. Ng, W. L. et al. Vat polymerization-based bioprinting—process, materials, applications and regulatory challenges. *Biofabrication* **12**, 022001 (2020).
42. Zhang, J. M. et al. Digital light processing based three-dimensional printing for medical applications. *International Journal of Bioprinting* **6**, 242 (2019).
43. Melchels, F. P. W., Feijen, J. & Grijpma, D. W. A review on stereolithography and its applications in biomedical engineering. *Biomaterials* **31**, 6121-6130 (2010).
44. Bártolo, P. J. Stereolithography: Materials, Processes and Applications. (Boston: Springer, 2011).
45. Skoog, S. A., Goering, P. L. & Narayan, R. J. Stereolithography in tissue engineering. *Journal of Materials Science:Materials in Medicine* **25**, 845-856 (2014).
46. Kruth, J. P. et al. Lasers and materials in selective laser sintering. *Assembly Automation* **23**, 357-371 (2003).
47. Agarwala, M. et al. Direct selective laser sintering of metals. *Rapid Prototyping Journal* **1**, 26-36 (1995).
48. Mazzoli, A. Selective laser sintering in biomedical engineering. *Medical & Biological Engineering & Computing* **51**, 245-256 (2013).
49. Schafer, K. J. et al. Two-photon absorption cross-sections of common photoinitiators. *Journal of Photochemistry and Photobiology A:Chemistry* **162**, 497-502 (2004).
50. Gittard, S. D. et al. Fabrication of microscale medical devices by two-photon polymerization with multiple foci via a spatial light modulator. *Biomedical Optics Express* **2**, 3167-3178 (2011).
51. Ziaee, M. & Crane, N. B. Binder jetting: a review of process, materials, and methods. *Additive Manufacturing* **28**, 781-801 (2019).
52. Lebel, L. L. et al. Ultraviolet-assisted direct-write fabrication of carbon nanotube/polymer nanocomposite microcoils. *Advanced Materials* **22**, 592-596 (2010).
53. Farahani, R. D., Dubé, M. & Therriault, D. Three-dimensional printing of multifunctional nanocomposites: manufacturing techniques and applications. *Advanced Materials* **28**, 5794-5821 (2016).
54. Wu, T. et al. Additively manufacturing high-performance bismaleimide architectures with ultraviolet-assisted direct ink writing. *Materials & Design* **180**, 107947 (2019).
55. Guo, Y. X. et al. Direct ink writing of high performance architectured polyimides with low dimensional shrinkage. *Advanced Engineering Materials* **21**, 1801314 (2019).
56. Ashwin, A. J. & Jafferson, J. M. State of the art direct ink writing (DIW) and experimental trial on DIW of HAp bio-ceramics. *Materials Today:Proceedings* **46**, 1298-1307 (2021).
57. Zhu, J. Z. et al. 3D printing of multi-scalable structures via high penetration near-infrared photopolymerization. *Nature Communications* **11**, 3462 (2020).
58. Liu, W. F., Song, H. W. & Huang, C. G. Maximizing mechanical properties and minimizing support material of PolyJet fabricated 3D lattice structures. *Additive Manufacturing* **35**, 101257 (2020).
59. Yusupov, V. et al. Laser-induced forward transfer hydrogel printing: a defined route for highly controlled process. *International Journal of Bioprinting* **6**, 271 (2020).
60. Ionita, C. N. et al. Challenges and limitations of patient-specific vascular phantom fabrication using 3D Polyjet printing. Proceedings of 9038 SPIE, Medical Imaging 2014: Biomedical Applications in Molecular, Structural, and Functional Imaging. San Diego, California, United States: SPIE, 2014, 90380M.
61. Pugalendhi, A., Ranganathan, R. & Chandrasekaran, M. Effect of process parameters on mechanical properties of VeroBlue material and their optimal selection in PolyJet technology. *The International Journal of Advanced Manufacturing Technology* **108**, 1049-1059 (2019).
62. Ibrahim, D. et al. Dimensional error of selective laser sintering, three-dimensional printing and PolyJet™ models in the reproduction of mandibular anatomy. *Journal of Cranio-Maxillofacial Surgery* **37**, 167-173 (2009).
63. Gaynor, A. T. et al. Multiple-material topology optimization of compliant mechanisms created via PolyJet three-dimensional printing. *Journal of Manufacturing Science and Engineering* **136**, 061015 (2014).
64. Meisel, N. A., Elliott, A. M. & Williams, C. B. A procedure for creating actuated joints via embedding shape memory alloys in PolyJet 3D printing. *Journal of Intelligent Material Systems and Structures* **26**, 1498-1512 (2015).
65. Childs, E. H. et al. Additive assembly for polyjet-based multi-material 3D printed microfluidics. *Journal of Microelectromechanical Systems*

29, 1094-1096 (2020).
66. Hull, C. W. The birth of 3D printing. *Research-Technology Management* **58**, 25-30 (2015).
67. Gross, B. C. et al. Evaluation of 3D printing and its potential impact on biotechnology and the chemical sciences. *Analytical Chemistry* **86**, 3240-3253 (2014).
68. He, Y. et al. Developments of 3D printing microfluidics and applications in chemistry and biology: a review. *Electroanalysis* **28**, 1658-1678 (2016).
69. Bártolo, P. J. & Gibson, I. History of stereolithographic processes. in Stereolithography: Materials, Processes and Applications (ed Bártolo, P. J.) (Boston: Springer, 2011), 37-56.
70. Waldbaur, A. et al. Let there be chip—towards rapid prototyping of microfluidic devices: one-step manufacturing processes. *Analytical Methods* **3**, 2681-2716 (2011).
71. Gizmo 3D Printers. The differences between bottom-up resin 3D printers and top-down resin 3D printers. (2020). at https://www.gizmo3dprinters.com.au/post/the-differences-between-bottom-up-resin-3d-printers-and-top-down-resin-3d-printers.
72. Han, L. H. et al. Projection microfabrication of three-dimensional scaffolds for tissue engineering. *Journal of Manufacturing Science and Engineering* **130**, 021005 (2008).
73. Choi, J. W. et al. Fabrication of 3D biocompatible/biodegradable micro-scaffolds using dynamic mask projection microstereolithography. *Journal of Materials Processing Technology* **209**, 5494-5503 (2009).
74. Pan, Y. Y., Zhou, C. & Chen, Y. Rapid manufacturing in minutes: the development of a mask projection stereolithography process for high-speed fabrication. Proceedings of the ASME 2012 International Manufacturing Science and Engineering Conference Collocated with the 40th North American Manufacturing Research Conference and in participation with the International Conference on Tribology Materials and Processing. Notre Dame, Indiana, USA: American Society of Mechanical Engineers, 2012, MSEC2012-7232.
75. Lu, Y. et al. A digital micro-mirror device-based system for the microfabrication of complex, spatially patterned tissue engineering scaffolds. *Journal of Biomedical Materials Research Part A* **77A**, 396-405 (2006).
76. Ho, C. M. B. et al. Femtosecond-laser-based 3D printing for tissue engineering and cell biology applications. *ACS Biomaterials Science & Engineering* **3**, 2198-2214 (2017).
77. Sun, C. et al. Projection micro-stereolithography using digital micro-mirror dynamic mask. *Sensors and Actuators A:Physical* **121**, 113-120 (2005).
78. Zheng, X. Y. et al. Multiscale metallic metamaterials. *Nature Materials* **15**, 1100-1106 (2016).
79. Ge, Q. et al. Projection micro stereolithography based 3D printing and its applications. *International Journal of Extreme Manufacturing* **2**, 022004 (2020).
80. Yang, Y. et al. 3D-printed biomimetic super-hydrophobic structure for microdroplet manipulation and oil/water separation. *Advanced Materials* **30**, 1704912 (2018).
81. Bhanvadia, A. A. et al. High-resolution stereolithography using a static liquid constrained interface. *Communications Materials* **2**, 41 (2021).
82. Walker, D. A., Hedrick, J. L. & Mirkin, C. A. Rapid, large-volume, thermally controlled 3D printing using a mobile liquid interface. *Science* **366**, 360-364 (2019).
83. Emami, M. M., Barazandeh, F. & Yaghmaie, F. Scanning-projection based stereolithography: method and structure. *Sensors and Actuators A:Physical* **218**, 116-124 (2014).
84. Deckard, C. R. & McClure, P. F. Selective laser sintering. (Doctoral dissertation, The University of Texas at Austin, 1988).
85. Williams, J. D. & Deckard, C. R. Advances in modeling the effects of selected parameters on the SLS process. *Rapid Prototyping Journal* **4**, 90-100 (1998).
86. Vaezi, M., Seitz, H. & Yang, S. F. A review on 3D micro-additive manufacturing technologies. *The International Journal of Advanced Manufacturing Technology* **67**, 1721-1754 (2013).
87. Vyatskikh, A. et al. Additive manufacturing of 3D nano-architected metals. *Nature Communications* **9**, 593 (2018).
88. Behera, D. et al. Current challenges and potential directions towards precision microscale additive manufacturing–Part IV: future perspectives. *Precision Engineering* **68**, 197-205 (2021).
89. Chizari, S. et al. Current challenges and potential directions towards precision microscale additive manufacturing–Part III: energy induced deposition and hybrid electrochemical processes. *Precision Engineering* **68**, 174-186 (2021).
90. Roy, N. K. et al. A novel microscale selective laser sintering (μ-SLS) process for the fabrication of microelectronic parts. *Microsystems & Nanoengineering* **5**, 64 (2019).
91. Pham, D. T. & Gault, R. S. A comparison of rapid prototyping technologies. *International Journal of Machine Tools and Manufacture* **38**, 1257-1287 (1998).
92. Kauppila, I. The best SLS 3D printers in 2021 – buyer's guide. (2022). at https://all3dp.com/1/best-sls-3d-printer-desktop-industrial/#section-industrial-sls-3d-printers.
93. Chizari, S., Shaw, L. A. & Hopkins, J. B. Simultaneous printing and deformation of microsystems *via* two-photon lithography and holographic optical tweezers. *Materials Horizons* **6**, 350-355 (2019).
94. Guss, G. M. et al. Nanoscale surface tracking of laser material processing using phase shifting diffraction interferometry. *Optics Express* **22**, 14493-14504 (2014).
95. Pascall, A. J. et al. Light-Directed electrophoretic deposition: a new additive manufacturing technique for arbitrarily patterned 3D composites. *Advanced Materials* **26**, 2252-2256 (2014).
96. Takai, T., Nakao, H. & Iwata, F. Three-dimensional microfabrication using local electrophoresis deposition and a laser trapping technique. *Optics Express* **22**, 28109-28117 (2014).
97. Mattle, T. et al. Laser induced forward transfer aluminum layers: process investigation by time resolved imaging. *Applied Surface Science* **258**, 9352-9354 (2012).
98. Askari, M. Metamaterial fabrication using combined multiphoton polymerization and optical trapping. PhD thesis, University of Nottingham, Nottingham, 2017.
99. Forman, D. L., Cole, M. C. & McLeod, R. R. Radical diffusion limits to photoinhibited superresolution lithography. *Physical Chemistry Chemical Physics* **15**, 14862-14867 (2013).
100. Rumi, M. et al. Two-photon absorbing materials and two-photon-induced chemistry. in Photoresponsive Polymers I (eds Marder, S. R. & Lee, K. S.) (Berlin: Springer, 2008), 1-95.
101. Fischer, J. et al. Three-dimensional multi-photon direct laser writing with variable repetition rate. *Optics Express* **21**, 26244-26260 (2013).
102. Malinauskas, M. et al. Femtosecond visible light induced two-photon photopolymerization for 3D micro/nanostructuring in photoresists and photopolymers. *Lithuanian Journal of Physics* **50**, 201-207 (2010).
103. Kawata, S. et al. Finer features for functional microdevices. *Nature* **412**, 697-698 (2001).
104. Maruo, S., Nakamura, O. & Kawata, S. Three-dimensional microfabrication with two-photon-absorbed photopolymerization. *Optics Letters* **22**, 132-134 (1997).
105. Farsari, M. et al. Two-photon polymerization of an Eosin Y-sensitized acrylate composite. *Journal of Photochemistry and Photobiology A:Chemistry* **181**, 132-135 (2006).

106. Lim, T. W., Park, S. H. & Yang, D. Y. Contour offset algorithm for precise patterning in two-photon polymerization. *Microelectronic Engineering* **77**, 382-388 (2005).
107. Pearre, B. W. et al. Fast micron-scale 3D printing with a resonant-scanning two-photon microscope. *Additive Manufacturing* **30**, 100887 (2019).
108. Kato, J. I. et al. Multiple-spot parallel processing for laser micronanofabrication. *Applied Physics Letters* **86**, 044102 (2005).
109. Kelemen, L., Valkai, S. & Ormos, P. Parallel photopolymerisation with complex light patterns generated by diffractive optical elements. *Optics Express* **15**, 14488-14497 (2007).
110. Zandrini, T. et al. Multi-foci laser microfabrication of 3D polymeric scaffolds for stem cell expansion in regenerative medicine. *Scientific Reports* **9**, 11761 (2019).
111. Maibohm, C. et al. Multi-beam two-photon polymerization for fast large area 3D periodic structure fabrication for bioapplications. *Scientific Reports* **10**, 8740 (2020).
112. Cheng, J. Y. et al. High-speed femtosecond laser beam shaping based on binary holography using a digital micromirror device. *Optics Letters* **40**, 4875-4878 (2015).
113. Lee, W. H. Binary synthetic holograms. *Applied Optics* **13**, 1677-1682 (1974).
114. Geng, Q. et al. Digital micromirror device-based two-photon microscopy for three-dimensional and random-access imaging. *Optica* **4**, 674-677 (2017).
115. Geng, Q. et al. Ultrafast multi-focus 3-D nano-fabrication based on two-photon polymerization. *Nature Communications* **10**, 2179 (2019).
116. Bertsch, A. et al. Microstereophotolithography using a liquid crystal display as dynamic mask-generator. *Microsystem Technologies* **3**, 42-47 (1997).
117. Zhu, G. H. et al. Simultaneous spatial and temporal focusing of femtosecond pulses. *Optics Express* **13**, 2153-2159 (2005).
118. Oron, D., Tal, E. & Silberberg, Y. Scanningless depth-resolved microscopy. *Optics Express* **13**, 1468-1476 (2005).
119. Kim, D. & So, P. T. C. High-throughput three-dimensional lithographic microfabrication. *Optics Letters* **35**, 1602-1604 (2010).
120. Yih, J. N. et al. Temporal focusing-based multiphoton excitation microscopy via digital micromirror device. *Optics Letters* **39**, 3134-3137 (2014).
121. Saha, S. K. et al. Scalable submicrometer additive manufacturing. *Science* **366**, 105-109 (2019).
122. Shusteff, M. et al. One-step volumetric additive manufacturing of complex polymer structures. *Science Advances* **3**, eaao5496 (2017).
123. Kelly, B. E. et al. Volumetric additive manufacturing via tomographic reconstruction. *Science* **363**, 1075-1079 (2019).
124. Loterie, D., Delrot, P. & Moser, C. High-resolution tomographic volumetric additive manufacturing. *Nature Communications* **11**, 852 (2020).
125. Regehly, M. et al. Xolography for linear volumetric 3D printing. *Nature* **588**, 620-624 (2020).
126. Liu, C., Xia, Z. & Czernuszka, J. T. Design and development of three-dimensional scaffolds for tissue engineering. *Chemical Engineering Research and Design* **85**, 1051-1064 (2007).
127. Hollister, S. J. Porous scaffold design for tissue engineering. *Nature Materials* **4**, 518-524 (2005).
128. Melchels, F. P. W. et al. Mathematically defined tissue engineering scaffold architectures prepared by stereolithography. *Biomaterials* **31**, 6909-6916 (2010).
129. Trachtenberg, J. E., Kasper, F. K. & Mikos, A. G. Polymer scaffold fabrication. in Principles of Tissue Engineering 4th edn (eds Lanza, R., Langer, R. & Vacanti, J.) (Amsterdam: Academic Press, 2014), 423-440.
130. Antonov, E. N. et al. Three-dimensional bioactive and biodegradable scaffolds fabricated by surface-selective laser sintering. *Advanced Materials* **17**, 327-330 (2005).
131. Nag, S., Banerjee, R. & Fraser, H. L. A novel combinatorial approach for understanding microstructural evolution and its relationship to mechanical properties in metallic biomaterials. *Acta Biomaterialia* **3**, 369-376 (2007).
132. Yang, K. et al. Bio-functional design, application and trends in metallic biomaterials. *International Journal of Molecular Sciences* **19**, 24 (2018).
133. Wilson, J. Metallic biomaterials: state of the art and new challenges. in Fundamental Biomaterials: Metals (eds Balakrishnan, P., Sreekala, M. S. & Thomas, S.) (Duxford: Woodhead Publishing, 2018), 1-33.
134. Ni, J. et al. Three-dimensional printing of metals for biomedical applications. *Materials Today Bio* **3**, 100024 (2019).
135. Chou, D. T. et al. Novel processing of iron–manganese alloy-based biomaterials by inkjet 3-D printing. *Acta Biomaterialia* **9**, 8593-8603 (2013).
136. Warnke, P. H. et al. Rapid prototyping: porous titanium alloy scaffolds produced by selective laser melting for bone tissue engineering. *Tissue Engineering Part C:Methods* **15**, 115-124 (2009).
137. Ngo, T. D. et al. Additive manufacturing (3D printing): a review of materials, methods, applications and challenges. *Composites Part B:Engineering* **143**, 172-196 (2018).
138. Zhang, W. Y., Tong, M. M. & Harrison, N. M. Resolution, Energy and time dependency on layer scaling in finite element modelling of laser beam powder bed fusion additive manufacturing. *Additive Manufacturing* **28**, 610-620 (2019).
139. Shahrubudin, N., Lee, T. C. & Ramlan, R. An overview on 3D printing technology: technological, materials, and applications. *Procedia Manufacturing* **35**, 1286-1296 (2019).
140. Alvarez, K. & Nakajima, H. Metallic scaffolds for bone regeneration. *Materials* **2**, 790-832 (2009).
141. Lin, H. M. et al. Scaffold 3D-printed from metallic nanoparticles-containing ink simultaneously eradicates tumor and repairs tumor-associated bone defects. *Small Methods* **5**, 2100536 (2021).
142. Munir, K. S., Li, Y. & Wen, C. Metallic scaffolds manufactured by selective laser melting for biomedical applications. in Metallic Foam Bone: Processing, Modification and Characterization and Properties (ed Wen, C.) (Amsterdam: Woodhead Publishing, 2017), 1-23.
143. Witte, F. et al. Cartilage repair on magnesium scaffolds used as a subchondral bone replacement. *Materialwissenschaft und Werkstofftechnik* **37**, 504-508 (2006).
144. Witte, F. et al. Biodegradable magnesium scaffolds: part II: peri-implant bone remodeling. *Journal of Biomedical Materials Research Part A* **81A**, 757-765 (2007).
145. Bottino, M. C. et al. Processing, characterization, and *in vitro/in vivo* evaluations of powder metallurgy processed Ti-13Nb-13Zr alloys. *Journal of Biomedical Materials Research Part A* **88A**, 689-696 (2009).
146. Long, W. J. & Scuderi, G. R. Porous tantalum cones for large metaphyseal tibial defects in revision total knee arthroplasty: a minimum 2-year follow-up. *The Journal of Arthroplasty* **24**, 1086-1092 (2009).
147. Wang, Y. et al. Superelastic cage implantation: a new technique for treating osteonecrosis of the femoral head with mid-term follow-ups. *The Journal of Arthroplasty* **24**, 1006-1014 (2009).
148. Zhang, L. C. et al. Manufacture by selective laser melting and mechanical behavior of a biomedical Ti–24Nb–4Zr–8Sn alloy. *Scripta Materialia* **65**, 21-24 (2011).
149. Lashneva, V. V., Kryuchkov, Y. N. & Sokhan, S. V. Bioceramics based on aluminum oxide. *Glass and Ceramics* **55**, 357-359 (1998).
150. Barone, D. T. J., Raquez, J. M. & Dubois, P. Bone-guided regeneration:

from inert biomaterials to bioactive polymer (nano)composites. *Polymers for Advanced Technologies* **22**, 463-475 (2011).
151. Rahaman, M. N. et al. Ceramics for prosthetic hip and knee joint replacement. *Journal of the American Ceramic Society* **90**, 1965-1988 (2007).
152. Lejeune, M. et al. Ink-jet printing of ceramic micro-pillar arrays. *Journal of the European Ceramic Society* **29**, 905-911 (2009).
153. Wu, L., Lin, L. J. & Qin, Y. X. Enhancement of cell ingrowth, proliferation, and early differentiation in a three-dimensional silicon carbide scaffold using low-intensity pulsed ultrasound. *Tissue Engineering Part A* **21**, 53-61 (2015).
154. Tripathi, G. & Basu, B. A porous hydroxyapatite scaffold for bone tissue engineering: physico-mechanical and biological evaluations. *Ceramics International* **38**, 341-349 (2012).
155. Shuai, C. et al. Graphene-reinforced mechanical properties of calcium silicate scaffolds by laser sintering. *RSC Advances* **4**, 12782-12788 (2014).
156. Dávila, J. L. et al. Fabrication of PCL/β-TCP scaffolds by 3D mini-screw extrusion printing. *Journal of Applied Polymer Science* **133**, 43031 (2016).
157. Son, J. S. et al. Porous hydroxyapatite scaffold with three-dimensional localized drug delivery system using biodegradable microspheres. *Journal of Controlled Release* **153**, 133-140 (2011).
158. Ma, J., Wang, C. & Peng, K. W. Electrophoretic deposition of porous hydroxyapatite scaffold. *Biomaterials* **24**, 3505-3510 (2003).
159. Shao, H. P. et al. 3D gel-printing of hydroxyapatite scaffold for bone tissue engineering. *Ceramics International* **45**, 1163-1170 (2019).
160. Scalera, F. et al. Development and characterization of UV curable epoxy/hydroxyapatite suspensions for stereolithography applied to bone tissue engineering. *Ceramics International* **40**, 15455-15462 (2014).
161. Chen, Z. W. et al. 3D printing of ceramics: a review. *Journal of the European Ceramic Society* **39**, 661-687 (2019).
162. Song, X. H. et al. Selective laser sintering of aliphatic-polycarbonate/hydroxyapatite composite scaffolds for medical applications. *The International Journal of Advanced Manufacturing Technology* **81**, 15-25 (2015).
163. Lewis, J. A. Direct-write assembly of ceramics from colloidal inks. *Current Opinion in Solid State and Materials Science* **6**, 245-250 (2002).
164. Simon, J. L. et al. *In vivo* bone response to 3D periodic hydroxyapatite scaffolds assembled by direct ink writing. *Journal of Biomedical Materials Research Part A* **83A**, 747-758 (2007).
165. Gerhardt, L. C. & Boccaccini, A. R. Bioactive glass and glass-ceramic scaffolds for bone tissue engineering. *Materials* **3**, 3867-3910 (2010).
166. Wen, Y. et al. 3D printed porous ceramic scaffolds for bone tissue engineering: a review. *Biomaterials Science* **5**, 1690-1698 (2017).
167. Ribas, R. G. et al. Current advances in bone tissue engineering concerning ceramic and bioglass scaffolds: a review. *Ceramics International* **45**, 21051-21061 (2019).
168. Wang, X. Y. et al. Biomaterial-based microstructures fabricated by two-photon polymerization microfabrication technology. *RSC Advances* **9**, 34472-34480 (2019).
169. Chen, G. P., Ushida, T. & Tateishi, T. Scaffold design for tissue engineering. *Macromolecular Bioscience* **2**, 67-77 (2002).
170. Deb, P. et al. Scaffold development using biomaterials: a review. *Materials Today:Proceedings* **5**, 12909-12919 (2018).
171. Liu, X. H. & Ma, P. X. Polymeric scaffolds for bone tissue engineering. *Annals of Biomedical Engineering* **32**, 477-486 (2004).
172. Hutmacher, D. W. Scaffolds in tissue engineering bone and cartilage. *Biomaterials* **21**, 2529-2543 (2000).
173. Calori, I. R. et al. Polymer scaffolds as drug delivery systems. *European Polymer Journal* **129**, 109621 (2020).
174. Kamoun, E. A., Kenawy, E. R. S. & Chen, X. A review on polymeric hydrogel membranes for wound dressing applications: PVA-based hydrogel dressings. *Journal of Advanced Research* **8**, 217-233 (2017).
175. Zhao, Y. et al. Preparation of nanofibers with renewable polymers and their application in wound dressing. *International Journal of Polymer Science* **2016**, 4672839 (2016).
176. Boni, R. et al. Current and novel polymeric biomaterials for neural tissue engineering. *Journal of Biomedical Science* **25**, 90 (2018).
177. Zhang, Q. Z. et al. Polymer scaffolds facilitate spinal cord injury repair. *Acta Biomaterialia* **88**, 57-77 (2019).
178. Urciuolo, A. et al. Intravital three-dimensional bioprinting. *Nature Biomedical Engineering* **4**, 901-915 (2020).
179. Weems, A. C. et al. 4D polycarbonates via stereolithography as scaffolds for soft tissue repair. *Nature Communications* **12**, 3771 (2021).
180. Nikolova, M. P. & Chavali, M. S. Recent advances in biomaterials for 3D scaffolds: a review. *Bioactive Materials* **4**, 271-292 (2019).
181. Hribar, K. C. et al. Light-assisted direct-write of 3D functional biomaterials. *Lab on A Chip* **14**, 268-275 (2014).
182. Drury, J. L. & Mooney, D. J. Hydrogels for tissue engineering: scaffold design variables and applications. *Biomaterials* **24**, 4337-4351 (2003).
183. Irawan, V. et al. Collagen scaffolds in cartilage tissue engineering and relevant approaches for future development. *Tissue Engineering and Regenerative Medicine* **15**, 673-697 (2018).
184. Soucy, J. R. et al. Photocrosslinkable gelatin/tropoelastin hydrogel adhesives for peripheral nerve repair. *Tissue Engineering Part A* **24**, 1393-1405 (2018).
185. Copes, F. et al. Collagen-based tissue engineering strategies for vascular medicine. *Frontiers in Bioengineering and Biotechnology* **7**, 166 (2019).
186. Liu, Y. X. & Chan-Park, M. B. Hydrogel based on interpenetrating polymer networks of dextran and gelatin for vascular tissue engineering. *Biomaterials* **30**, 196-207 (2009).
187. Feng, Q. et al. Dynamic and cell-infiltratable hydrogels as injectable carrier of therapeutic cells and drugs for treating challenging bone defects. *ACS Central Science* **5**, 440-450 (2019).
188. Xu, J. B. et al. Injectable stem cell-laden supramolecular hydrogels enhance in situ osteochondral regeneration via the sustained co-delivery of hydrophilic and hydrophobic chondrogenic molecules. *Biomaterials* **210**, 51-61 (2019).
189. Osidak, E. O. et al. Collagen as bioink for bioprinting: a comprehensive review. *International Journal of Bioprinting* **6**, 270 (2020).
190. Lee, J. M. et al. Bioprinting of collagen: considerations, potentials, and applications. *Macromolecular Bioscience* **21**, 2000280 (2021).
191. Rajabi, N. et al. Recent advances on bioprinted gelatin methacrylate-based hydrogels for tissue repair. *Tissue Engineering Part A* **27**, 679-702 (2021).
192. Collins, M. N. & Birkinshaw, C. Hyaluronic acid based scaffolds for tissue engineering-a review. *Carbohydrate Polymers* **92**, 1262-1279 (2013).
193. Chircov, C., Grumezescu, A. M. & Bejenaru, L. E. Hyaluronic acid-based scaffolds for tissue engineering. *Romanian Journal of Morphology and Embryology* **59**, 71-76 (2018).
194. Yoo, H. S. et al. Hyaluronic acid modified biodegradable scaffolds for cartilage tissue engineering. *Biomaterials* **26**, 1925-1933 (2005).
195. Rakin, R. H. et al. Tunable metacrylated hyaluronic acid-based hybrid bioinks for stereolithography 3D bioprinting. *Biofabrication* **13**, 044109 (2021).
196. Hernández-González, A. C., Téllez-Jurado, L. & Rodríguez-Lorenzo, L. M. Alginate hydrogels for bone tissue engineering, from injectables to bioprinting: a review. *Carbohydrate Polymers* **229**, 115514 (2020).

197. Arya, N. et al. RGDSP functionalized carboxylated agarose as extrudable carriers for chondrocyte delivery. *Materials Science and Engineering:C* **99**, 103-111 (2019).
198. Norotte, C. et al. Scaffold-free vascular tissue engineering using bioprinting. *Biomaterials* **30**, 5910-5917 (2009).
199. Mallakpour, S., Sirous, F. & Hussain, C. M. Current achievements in 3D bioprinting technology of chitosan and its hybrids. *New Journal of Chemistry* **45**, 10565-10576 (2021).
200. Prestwich, G. D. Hyaluronic acid-based clinical biomaterials derived for cell and molecule delivery in regenerative medicine. *Journal of Controlled Release* **155**, 193-199 (2011).
201. Zhai, X. Y. et al. 3D-Bioprinted osteoblast-laden nanocomposite hydrogel constructs with induced microenvironments promote cell viability, differentiation, and osteogenesis both in vitro and in vivo. *Advanced Science* **5**, 1700550 (2018).
202. Wang, Z. J. et al. Visible light photoinitiation of cell-adhesive gelatin methacryloyl hydrogels for stereolithography 3D bioprinting. *ACS Applied Materials & Interfaces* **10**, 26859-26869 (2018).
203. Mondschein, R. J. et al. Polymer structure-property requirements for stereolithographic 3D printing of soft tissue engineering scaffolds. *Biomaterials* **140**, 170-188 (2017).
204. Liao, C. Z., Wuethrich, A. & Trau, M. A material odyssey for 3D nano/microstructures: two photon polymerization based nanolithography in bioapplications. *Applied Materials Today* **19**, 100635 (2020).
205. Song, J. X. et al. From simple to architecturally complex hydrogel scaffolds for cell and tissue engineering applications: opportunities presented by two-photon polymerization. *Advanced Healthcare Materials* **9**, 1901217 (2020).
206. Lam, T. et al. Photopolymerizable gelatin and hyaluronic acid for stereolithographic 3D bioprinting of tissue-engineered cartilage. *Journal of Biomedical Materials Research Part B:Applied Biomaterials* **107**, 2649-2657 (2019).
207. Highley, C. B., Rodell, C. B. & Burdick, J. A. Direct 3D printing of shear-thinning hydrogels into self-healing hydrogels. *Advanced Materials* **27**, 5075-5079 (2015).
208. Koroleva, A. et al. Two-photon polymerization-generated and micromolding-replicated 3D scaffolds for peripheral neural tissue engineering applications. *Biofabrication* **4**, 025005 (2012).
209. Weiß, T. et al. Two-photon polymerization of biocompatible photopolymers for microstructured 3D biointerfaces. *Advanced Engineering Materials* **13**, B264-B273 (2011).
210. Timashev, P. et al. Novel biodegradable star-shaped polylactide scaffolds for bone regeneration fabricated by two-photon polymerization. *Nanomedicine* **11**, 1041-1053 (2016).
211. Gao, W. et al. Ionic carbazole-based water-soluble two-photon photoinitiator and the fabrication of biocompatible 3D hydrogel scaffold. *ACS Applied Materials & Interfaces* **13**, 27796-27805 (2021).
212. Cheung, H. Y. et al. A critical review on polymer-based bio-engineered materials for scaffold development. *Composites Part B:Engineering* **38**, 291-300 (2007).
213. Eltom, A., Zhong, G. Y. & Muhammad, A. Scaffold techniques and designs in tissue engineering functions and purposes: a review. *Advances in Materials Science and Engineering* **2019**, 3429527 (2019).
214. Place, E. S. et al. Synthetic polymer scaffolds for tissue engineering. *Chemical Society Reviews* **38**, 1139-1151 (2009).
215. Janoušková, O. Synthetic polymer scaffolds for soft tissue engineering. *Physiological Research* **67**, S335-S348 (2018).
216. Zhu, J. M. & Marchant, R. E. Design properties of hydrogel tissue-engineering scaffolds. *Expert Review of Medical Devices* **8**, 607-626 (2011).
217. Platel, R. H., Hodgson, L. M. & Williams, C. K. Biocompatible initiators for lactide polymerization. *Polymer Reviews* **48**, 11-63 (2008).
218. Zhang, W. D. et al. Tuning the poisson's ratio of biomaterials for investigating cellular response. *Advanced Functional Materials* **23**, 3226-3232 (2013).
219. Lunzer, M. et al. A modular approach to sensitized two-photon patterning of photodegradable hydrogels. *Angewandte Chemie International Edition* **57**, 15122-15127 (2018).
220. Do, A. V. et al. Controlled drug delivery from 3D printed two-photon polymerized poly(ethylene glycol) dimethacrylate devices. *International Journal of Pharmaceutics* **552**, 217-224 (2018).
221. Richter, B. et al. Guiding cell attachment in 3D microscaffolds selectively functionalized with two distinct adhesion proteins. *Advanced Materials* **29**, 1604342 (2017).
222. Gou, X. R. et al. Mechanical property of PEG hydrogel and the 3D red blood cell microstructures fabricated by two-photon polymerization. *Applied Surface Science* **416**, 273-280 (2017).
223. Kufelt, O. et al. Hyaluronic acid based materials for scaffolding via two-photon polymerization. *Biomacromolecules* **15**, 650-659 (2014).
224. Ulery, B. D., Nair, L. S. & Laurencin, C. T. Biomedical applications of biodegradable polymers. *Journal of Polymer Science Part B:Polymer Physics* **49**, 832-864 (2011).
225. Pok, S. & Jacot, J. G. Biomaterials advances in patches for congenital heart defect repair. *Journal of Cardiovascular Translational Research* **4**, 646-654 (2011).
226. Prabhakaran, M. P. et al. Biomimetic material strategies for cardiac tissue engineering. *Materials Science and Engineering:C* **31**, 503-513 (2011).
227. Shin, J. H. et al. Evaluation of cell proliferation and differentiation on a poly(propylene fumarate) 3D scaffold treated with functional peptides. *Journal of Materials Science* **46**, 5282-5287 (2011).
228. Spiller, K. L., Maher, S. A. & Lowman, A. M. Hydrogels for the repair of articular cartilage defects. *Tissue Engineering Part B:Review* **17**, 281-299 (2011).
229. Tang, X. Y. et al. Polymeric biomaterials in tissue engineering and regenerative medicine. in Natural and Synthetic Biomedical Polymers (eds Kumbar, S. G., Laurencin, C. T. & Deng, M.) (Amsterdam: Elsevier, 2014), 351-371.
230. Chen, Q., Roether, J. A. & Boccaccini, A. R. Tissue engineering scaffolds from bioactive glass and composite materials. *Topics in Tissue Engineering* **4**, 1-27 (2008).
231. Boccaccini, A. R. & Blaker, J. J. Bioactive composite materials for tissue engineering scaffolds. *Expert Review of Medical Devices* **2**, 303-317 (2005).
232. Qu, H. W. et al. Biomaterials for bone tissue engineering scaffolds: a review. *RSC Advances* **9**, 26252-26262 (2019).
233. Shapiro, J. M. & Oyen, M. L. Hydrogel composite materials for tissue engineering scaffolds. *JOM* **65**, 505-516 (2013).
234. Bhaskar, B. et al. Biomaterials in Tissue Engineering and Regenerative Medicine: from Basic Concepts to State of the Art Approaches. (Singapore: Springer, 2021).
235. Narayan, R. ASM Handbook, Volume 23: Materials for Medical Devices. (Materials Park: ASM International, 2012).
236. Jani, J. M. et al. A review of shape memory alloy research, applications and opportunities. *Materials & Design* (*1980-2015*) **56**, 1078-1113 (2014).
237. Mirzababaei, S. & Pasebani, S. A review on binder jet additive manufacturing of 316L stainless steel. *Journal of Manufacturing and Materials Processing* **3**, 82 (2019).
238. Hofer, A. K. et al. Effect of binder system on the thermophysical properties of 3D-printed zirconia ceramics. *International Journal of Applied Ceramic Technology* **19**, 174-180 (2022).
239. Desponds, A. et al. 3D printing and pyrolysis of optical ZrO_2

nanostructures by two-photon lithography: reduced shrinkage and crystallization mediated by nanoparticles seeds. *Small* **17**, 2102486 (2021).
240. Niu, Y. Q. et al. HA-coated collagen nanofibers for urethral regeneration via in situ polarization of M2 macrophages. *Journal of Nanobiotechnology* **19**, 283 (2021).
241. Sun, K. et al. Silk fibroin/collagen and silk fibroin/chitosan blended three-dimensional scaffolds for tissue engineering. *European Journal of Orthopaedic Surgery & Traumatology* **25**, 243-249 (2015).
242. Wang, S. B. et al. Three dimensional printing bilayer membrane scaffold promotes wound healing. *Frontiers in Bioengineering and Biotechnology* **7**, 348 (2019).
243. Selim, O. A. et al. Three-dimensional engineered peripheral nerve: toward a new era of patient-specific nerve repair solutions. *Tissue Engineering Part B: Reviews*. http://dx.doi.org/10.1089/ten.TEB.2020.0355 (2021).
244. Morimoto, T. K. et al. Toward the design of personalized continuum surgical robots. *Annals of Biomedical Engineering* **46**, 1522-1533 (2018).
245. Yuan, H. B., Xing, K. & Hsu, H. Y. Trinity of three-dimensional (3D) scaffold, vibration, and 3D printing on cell culture application: a systematic review and indicating future direction. *Bioengineering* **5**, 57 (2018).
246. Greiner, A. M., Richter, B. & Bastmeyer, M. Micro-engineered 3D scaffolds for cell culture studies. *Macromolecular Bioscience* **12**, 1301-1314 (2012).
247. Hippler, M. et al. 3D scaffolds to study basic cell biology. *Advanced Materials* **31**, 1808110 (2019).
248. Kim, K. et al. Stereolithographic bone scaffold design parameters: osteogenic differentiation and signal expression. *Tissue Engineering Part B:Reviews* **16**, 523-539 (2010).
249. Chen, Q. H. et al. A study on biosafety of HAP ceramic prepared by SLA-3D printing technology directly. *Journal of the Mechanical Behavior of Biomedical Materials* **98**, 327-335 (2019).
250. Liu, F. H. Synthesis of biomedical composite scaffolds by laser sintering: mechanical properties and *in vitro* bioactivity evaluation. *Applied Surface Science* **297**, 1-8 (2014).
251. Putra, N. E. et al. Extrusion-based 3D printed biodegradable porous iron. *Acta Biomaterialia* **121**, 741-756 (2021).
252. Ricci, D. et al. Scaling-up techniques for the nanofabrication of cell culture substrates via two-photon polymerization for industrial-scale expansion of stem cells. *Materials* **10**, 66 (2017).
253. Lemma, E. D. et al. Microenvironmental stiffness of 3D polymeric structures to study invasive rates of cancer cells. *Advanced Healthcare Materials* **6**, 1700888 (2017).
254. Rovira, D. S. et al. Additive manufacturing of polymeric scaffolds for biomimetic cell membrane engineering. *Materials & Design* **201**, 109486 (2021).
255. Pandey, M. et al. 3D printing for oral drug delivery: a new tool to customize drug delivery. *Drug Delivery and Translational Research* **10**, 986-1001 (2020).
256. Prasad, L. K. & Smyth, H. 3D Printing technologies for drug delivery: a review. *Drug Development and Industrial Pharmacy* **42**, 1019-1031 (2016).
257. Wu, B. M. et al. Solid free-form fabrication of drug delivery devices. *Journal of Controlled Release* **40**, 77-87 (1996).
258. Khaled, S. A. et al. 3D extrusion printing of high drug loading immediate release paracetamol tablets. *International Journal of Pharmaceutics* **538**, 223-230 (2018).
259. Cui, M. S. et al. Fabrication of high drug loading levetiracetam tablets using semi-solid extrusion 3D printing. *Journal of Drug Delivery Science and Technology* **57**, 101683 (2020).
260. Robles-Martinez, P. et al. 3D printing of a multi-layered polypill containing six drugs using a novel stereolithographic method. *Pharmaceutics* **11**, 274 (2019).
261. Economidou, S. N. et al. 3D printed microneedle patches using stereolithography (SLA) for intradermal insulin delivery. *Materials Science and Engineering:C* **102**, 743-755 (2019).
262. Limongi, T. et al. Drug delivery applications of three-dimensional printed (3DP) mesoporous scaffolds. *Pharmaceutics* **12**, 851 (2020).
263. Ishack, S. et al. Bone regeneration in critical bone defects using three-dimensionally printed β-tricalcium phosphate/hydroxyapatite scaffolds is enhanced by coating scaffolds with either dipyridamole or BMP-2. *Journal of Biomedical Materials Research Part B:Applied Biomaterials* **105**, 366-375 (2017).
264. Rosenberg, M. et al. Bone morphogenic protein 2-loaded porous silicon carriers for osteoinductive implants. *Pharmaceutics* **11**, 602 (2019).
265. Saska, S. et al. Three-dimensional printing and in vitro evaluation of poly(3-hydroxybutyrate) scaffolds functionalized with osteogenic growth peptide for tissue engineering. *Materials Science and Engineering:C* **89**, 265-273 (2018).
266. Xu, Y. et al. Drug loading/release and bioactivity research of a mesoporous bioactive glass/polymer scaffold. *Ceramics International* **45**, 18003-18013 (2019).
267. Fang, J. H. et al. Transdermal composite microneedle composed of mesoporous iron oxide nanoraspberry and PVA for androgenetic alopecia treatment. *Polymers* **12**, 1392 (2020).
268. Amini, A. R., Laurencin, C. T. & Nukavarapu, S. P. Bone tissue engineering: recent advances and challenges. *Critical Reviews™ in Biomedical Engineering* **40**, 363-408 (2012).
269. Kang, H. W. et al. A 3D bioprinting system to produce human-scale tissue constructs with structural integrity. *Nature Biotechnology* **34**, 312-319 (2016).
270. Bahraminasab, M. Challenges on optimization of 3D-printed bone scaffolds. *BioMedical Engineering OnLine* **19**, 69 (2020).
271. Polo-Corrales, L., Latorre-Esteves, M. & Ramirez-Vick, J. E. Scaffold design for bone regeneration. *Journal of Nanoscience and Nanotechnology* **14**, 15-56 (2014).
272. Bendtsen, S. T., Quinnell, S. P. & Wei, M. Development of a novel alginate-polyvinyl alcohol-hydroxyapatite hydrogel for 3D bioprinting bone tissue engineered scaffolds. *Journal of Biomedical Materials Research Part A* **105**, 1457-1468 (2017).
273. Peltola, S. M. et al. A review of rapid prototyping techniques for tissue engineering purposes. *Annals of Medicine* **40**, 268-280 (2008).
274. Lee, K. W. et al. Poly(propylene fumarate) bone tissue engineering scaffold fabrication using stereolithography: effects of resin formulations and laser parameters. *Biomacromolecules* **8**, 1077-1084 (2007).
275. Roskies, M. et al. Improving PEEK bioactivity for craniofacial reconstruction using a 3D printed scaffold embedded with mesenchymal stem cells. *Journal of Biomaterials Applications* **31**, 132-139 (2016).
276. Du, Y. Y. et al. Selective laser sintering scaffold with hierarchical architecture and gradient composition for osteochondral repair in rabbits. *Biomaterials* **137**, 37-48 (2017).
277. An, J. et al. Advanced nanobiomaterial strategies for the development of organized tissue engineering constructs. *Nanomedicine* **8**, 591-602 (2013).
278. Maggi, A., Li, H. Q. & Greer, J. R. Three-dimensional nano-architected scaffolds with tunable stiffness for efficient bone tissue growth. *Acta Biomaterialia* **63**, 294-305 (2017).
279. Felfel, R. M. et al. Performance of multiphase scaffolds for bone repair based on two-photon polymerized poly(D, L-lactide-*co*-ε-

caprolactone), recombinamers hydrogel and nano-HA. *Materials & Design* **160**, 455-467 (2018).
280. Towler, D. A. The osteogenic-angiogenic interface: novel insights into the biology of bone formation and fracture repair. *Current Osteoporosis Reports* **6**, 67-71 (2008).
281. Qazi, T. H. et al. Extrusion printed scaffolds with varying pore size as modulators of MSC angiogenic paracrine effects. *ACS Biomaterials Science & Engineering* **5**, 5348-5358 (2019).
282. Cidonio, G. et al. Nanoclay-based 3D printed scaffolds promote vascular ingrowth *ex vivo* and generate bone mineral tissue *in vitro* and *in vivo*. *Biofabrication* **12**, 035010 (2020).
283. Santos, M. I. et al. Crosstalk between osteoblasts and endothelial cells co-cultured on a polycaprolactone–starch scaffold and the *in vitro* development of vascularization. *Biomaterials* **30**, 4407-4415 (2009).
284. Piard, C. et al. Bioprinted osteon-like scaffolds enhance *in vivo* neovascularization. *Biofabrication* **11**, 025013 (2019).
285. Piard, C. et al. 3D printed HUVECs/MSCs cocultures impact cellular interactions and angiogenesis depending on cell-cell distance. *Biomaterials* **222**, 119423 (2019).
286. Druecke, D. et al. Neovascularization of poly(ether ester) block-copolymer scaffolds *in vivo*: long-term investigations using intravital fluorescent microscopy. *Journal of Biomedical Materials Research Part A* **68A**, 10-18 (2004).
287. Rouwkema, J., Rivron, N. C. & van Blitterswijk, C. A. Vascularization in tissue engineering. *Trends in Biotechnology* **26**, 434-441 (2008).
288. Khang, G. Handbook of Intelligent Scaffolds for Tissue Engineering and Regenerative Medicine. (Singapore: Pan Stanford, 2012), 589-606.
289. Mobaraki, M. et al. Bioinks and bioprinting: a focused review. *Bioprinting* **18**, e00080 (2020).
290. Gopinathan, J. & Noh, I. Recent trends in bioinks for 3D printing. *Biomaterials Research* **22**, 11 (2018).
291. Bajaj, P. et al. 3D biofabrication strategies for tissue engineering and regenerative medicine. *Annual Review of Biomedical Engineering* **16**, 247-276 (2014).
292. Grinstaff, M. W. Dendritic macromers for hydrogel formation: tailored materials for ophthalmic, orthopedic, and biotech applications. *Journal of Polymer Science Part A:Polymer Chemistry* **46**, 383-400 (2008).
293. Gentsch, R. & Börner, H. G. Designing Three-Dimensional Materials at the Interface to Biology. in Bioactive Surfaces (eds Börner, H. G. & Lutz, J. F.) (Berlin: Springer, 2011), 163-192.
294. Koçak, E., Yıldız, A. & Acartürk, F. Three dimensional bioprinting technology: applications in pharmaceutical and biomedical area. *Colloids and Surfaces B:Biointerfaces* **197**, 111396 (2021).
295. Hockaday, L. A. et al. Rapid 3D printing of anatomically accurate and mechanically heterogeneous aortic valve hydrogel scaffolds. *Biofabrication* **4**, 035005 (2012).
296. Mohammadian, Y. & Nasirzadeh, N. Toxicity risks of occupational exposure in 3D printing and bioprinting industries: a systematic review. *Toxicology and Industrial Health* **37**, 573-584 (2021).
297. Amani, H. et al. Three-dimensional graphene foams: synthesis, properties, biocompatibility, biodegradability, and applications in tissue engineering. *ACS Biomaterials Science & Engineering* **5**, 193-214 (2019).
298. Macdonald, N. P. et al. Assessment of biocompatibility of 3D printed photopolymers using zebrafish embryo toxicity assays. *Lab on A Chip* **16**, 291-297 (2016).
299. He, H. Y. et al. Rapid prototyping for tissue-engineered bone scaffold by 3D printing and biocompatibility study. *International Journal of Clinical and Experimental Medicine* **8**, 11777-11785 (2015).
300. Liu, J. et al. Current advances and future perspectives of 3D printing natural-derived biopolymers. *Carbohydrate Polymers* **207**, 297-316 (2019).
301. HP jet fusion 3200 3D printer. at https://pick3dprinter.com/hp-jet-fusion-3200-review/.
302. Behera, D. et al. Current challenges and potential directions towards precision microscale additive manufacturing–part II: laser-based curing, heating, and trapping processes. *Precision Engineering* **68**, 301-318 (2021).
303. Nazir, A. & Jeng, J. Y. A high-speed additive manufacturing approach for achieving high printing speed and accuracy. *Proceedings of the Institution of Mechanical Engineers, Part C:Journal of Mechanical Engineering Science* **234**, 2741-2749 (2020).
304. FDM vs. SLA: compare the two most popular types of 3D printers. at https://formlabs.com/blog/fdm-vs-sla-compare-types-of-3d-printers/.
305. EOS P 500 The automation-ready manufacturing platform for laser sintering of plastic parts on an industrial scale. at https://www.eos.info/en/additive-manufacturing/3d-printing-plastic/eos-polymer-systems/eos-p-500.
306. SLS printer EOS formiga P 110 velocis. at https://www.eos.info/en/additive-manufacturing/3d-printing-plastic/eos-polymer-systems/formiga-p-110-velocis.
307. Desktop SLS printer red rock 3D. at http://www.redrocksls.com/.
308. Shallan, A. I. et al. Cost-effective three-dimensional printing of visibly transparent microchips within minutes. *Analytical Chemistry* **86**, 3124-3130 (2014).
309. Vizsnyiczai, G., Kelemen, L. & Ormos, P. Holographic multi-focus 3D two-photon polymerization with real-time calculated holograms. *Optics Express* **22**, 24217-24223 (2014).
310. Tagliaferri, V. et al. Environmental and economic analysis of FDM, SLS and MJF additive manufacturing technologies. *Materials* **12**, 4161 (2019).
311. Pati, F. et al. Printing three-dimensional tissue analogues with decellularized extracellular matrix bioink. *Nature Communications* **5**, 3935 (2014).
312. Kuang, X. et al. 3D printing of highly stretchable, shape-memory, and self-healing elastomer toward novel 4D printing. *ACS Applied Materials & Interfaces* **10**, 7381-7388 (2018).
313. Schmidleithner, C. & Kalaskar, D. M. Stereolithography. in 3D Printing (ed Cvetković, D.) (London: IntechOpen, 2018).
314. Stampfl, J. et al. Photopolymers with tunable mechanical properties processed by laser-based high-resolution stereolithography. *Journal of Micromechanics and Microengineering* **18**, 125014 (2008).
315. Weisgrab, G. et al. 3D Printing of large-scale and highly porous biodegradable tissue engineering scaffolds from poly(trimethylene-carbonate) using two-photon-polymerization. *Biofabrication* **12**, 045036 (2020).
316. Lamont, A. C. et al. A facile multi-material direct laser writing strategy. *Lab on A Chip* **19**, 2340-2345 (2019).